Journal of Structural Geology 31 (2009) 1472–1489

Contents lists available at ScienceDirect

Journal of Structural Geology

journal homepage: www.elsevier.com/locate/jsg

Kinematic analysis of serpentinite structures and the manifestation of transpression in southwestern Puerto Rico

Daniel A. Laó-Dávila*, Thomas H. Anderson

Department of Geology and Planetary Science, University of Pittsburgh, 200 SRCC, 4107 O'Hara Street, Pittsburgh, PA 15260-3332, United States

ARTICLE INFO

Article history:
Received 18 November 2008
Received in revised form
25 September 2009
Accepted 30 September 2009
Available online 14 October 2009

Keywords:
Eocene
Oblique faults
S–C
Strain

ABSTRACT

Faults and shear zones recorded in the Monte del Estado and Río Guanajibo serpentinite masses in southwestern Puerto Rico show previously unrecognized southwestward tectonic transport. The orientations of planar and linear structures and the sense of slip along faults and shear zones determined by offset rock layers, drag folds in foliations, and steps in slickensided surfaces and/or S–C fabrics from 1846 shear planes studied at more than 300 stations reveal two predominant groups of faults: 1) northwesterly-striking thrust faults and easterly-striking left-lateral faults and, 2) northwesterly-striking right-lateral faults and easterly-striking thrust faults. Shortening and extension (P and T) axes calculated for geographic domains within the serpentinite reveal early north-trending shortening followed by southwestward-directed movement during which older structures were re-activated. The SW-directed shortening is attributed to transpression that accompanied Late Eocene left-lateral shearing of the serpentinite. A third, younger, group comprising fewer faults consists of northwesterly-striking left-lateral faults and north-directed thrusts that also may be related to the latest transpressional deformation within Puerto Rico. Deformational events in Puerto Rico correlate to tectonic events along the Caribbean–North American plate boundary.

1. Introduction

Exposures of serpentinite in the Greater Antilles at the Caribbean–North America plate boundary zone attest to the complex tectonic history of the region (Fig. 1). Serpentinite crops out in northern Cuba, where it is part of serpentinite mélange thrust northward during multiple tectonic events beginning in the Early Cretaceous and ending in the Late Eocene (Draper and Barros, 1994; Cobiella-Reguera, 2005). Serpentinite in Hispaniola crops out in the Cordillera Central (Duarte–Loma Caribe) and North Coast belts and according to Bowin (1966), Nagle (1974), and Draper et al. (1996) was emplaced in the Aptian–early Albian and Paleocene, respectively. A small block of serpentinite is also exposed in the Blue Mountains of eastern Jamaica (Draper, 1979). In Puerto Rico, serpentinite in Sierra Bermeja along the southwestern margin of the island, has been classified as part of a serpentinite mélange because it contains pieces of Early Jurassic to Cretaceous chert, 120 My old amphibolite, metabasalt, schist, gneiss, and greenstone (Mattson, 1960; Tobisch, 1968; Montgomery et al., 1994; Schellekens, 1998).

The complex tectonic evolution of the Caribbean–North America plate boundary includes possible subduction polarity reversal, collisions, strike-slip faulting accompanied by contraction (transpression), and changes of slip along fault zones (Glover, 1971; Erikson et al., 1990; Pindell, 1994; Draper et al., 1996; Escuder-Viruete et al., 2006; García-Casco et al., 2008). Although many studies have described the spatial relationships, structural contacts, and stratigraphy of Caribbean serpentinite and related formations (e.g. Lewis et al., 2006), studies of the internal structure of serpentinite bodies are limited. A better understanding of the internal strain and deformation of serpentinite has the potential to provide new insights into the tectonic evolution of the Caribbean–North America plate boundary zone, which is commonly defined by regional strike-slip faults.

Within large strike-slip fault zones the combination of contraction and strike-slip deformation, called transpression, is common as it is in collisional orogenic belts, oblique subduction margins, restraining bends, and in slate belts (Harland, 1971; Dewey et al., 1998). Masses of serpentinite, which contain metamorphic blocks, may occur within transpressive zones (e.g. Bailey et al., 2000; Harlow et al., 2004; Mori and Ogawa, 2005).

The objectives of this study are to characterize the styles and processes of deformation of serpentinite bodies in western Puerto Rico, to constrain the age of deformation, and to unravel the

* Corresponding author. Fax: +1 787 265 1684.
E-mail address: daniel.lao@upr.edu (D.A. Laó-Dávila).

0191-8141/$ – see front matter © 2009 Elsevier Ltd. All rights reserved.
doi:10.1016/j.jsg.2009.09.008

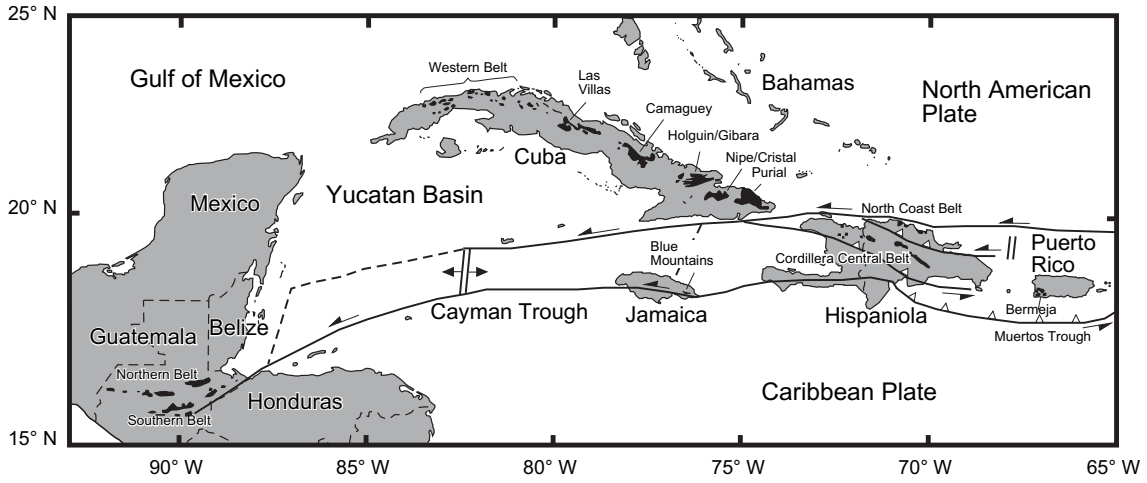

Fig. 1. Tectonic setting of the current northern plate boundary between the Caribbean and North American plates showing the distribution of ultramafic rocks including serpentinite (modified from Wadge et al., 1984).

tectonic history of some of the oldest rocks in the northeastern Caribbean plate boundary zone. Furthermore, this study aims to contribute to the understanding of serpentinite deformational structures (e.g. Wojtal and Mitra, 1988; Wojtal, 2001; Li et al., 2004; Andreani et al., 2005; Nozaka, 2005; Auzende et al., 2006) by describing deformed serpentinite from Puerto Rico.

2. Regional setting

2.1. Puerto Rico

Puerto Rico currently lies within the plate boundary zone between the Caribbean and North American plates (Fig. 1). The northern tectonic boundary of the island is characterized by highly oblique subduction as suggested by Global Positioning System studies (Jansma et al., 2000). The southern margin of Puerto Rico is delimited by the Muertos trough where underthrusting has been suggested to be currently occurring based on focal mechanisms of seismic events (Byrne et al., 1985). The island consists mainly of Cretaceous to Eocene volcanic and volcaniclastic rocks, limestone, and intrusive rocks (Fig. 2). Early Jurassic to Late Cretaceous ultramafic rocks crop out in the southwestern part (Montgomery et al., 1994), and gently dipping late Tertiary limestone strata crop out along the north and south coasts (Monroe, 1980). Two northwest-striking fault zones, the Northern Puerto Rico fault zone (NPRFZ) and the Southern Puerto Rico fault zone (SPRFZ), divide the island

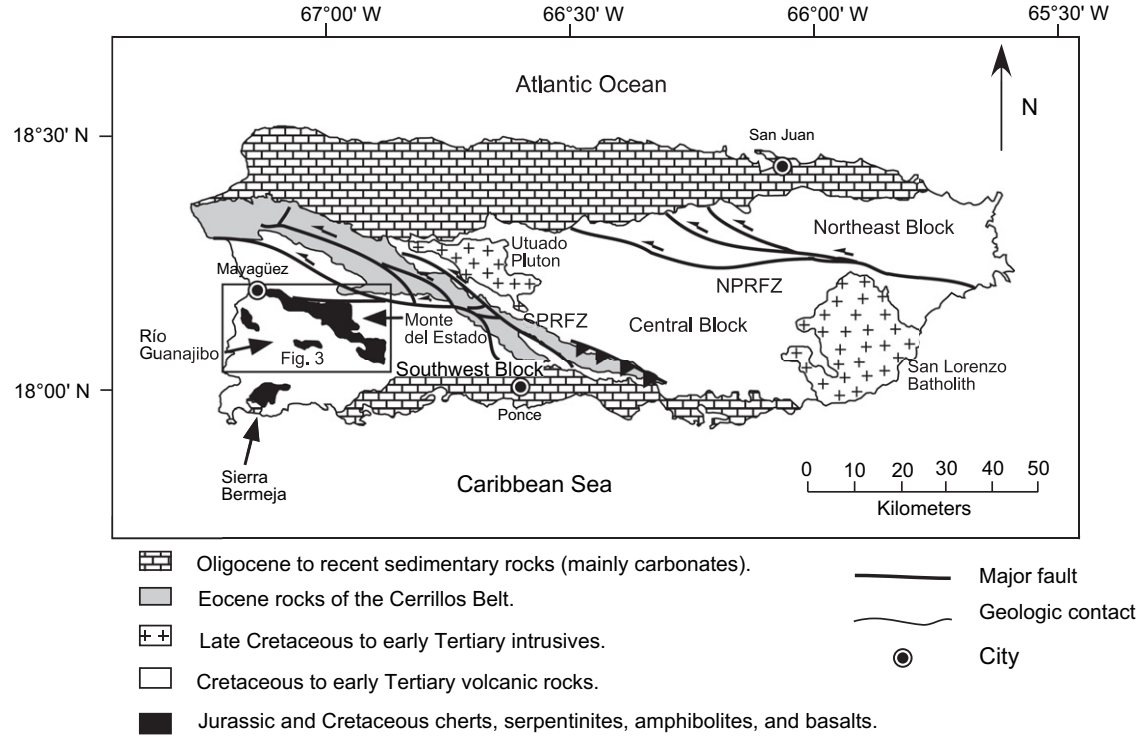

Fig. 2. Generalized geologic map of Puerto Rico showing location of serpentinite bodies and major fault zones. The Southern Puerto Rico fault zone (SPRFZ) and the Northern Puerto Rico fault zone (NPRFZ) separate the island into three blocks (modified from Monroe, 1980).

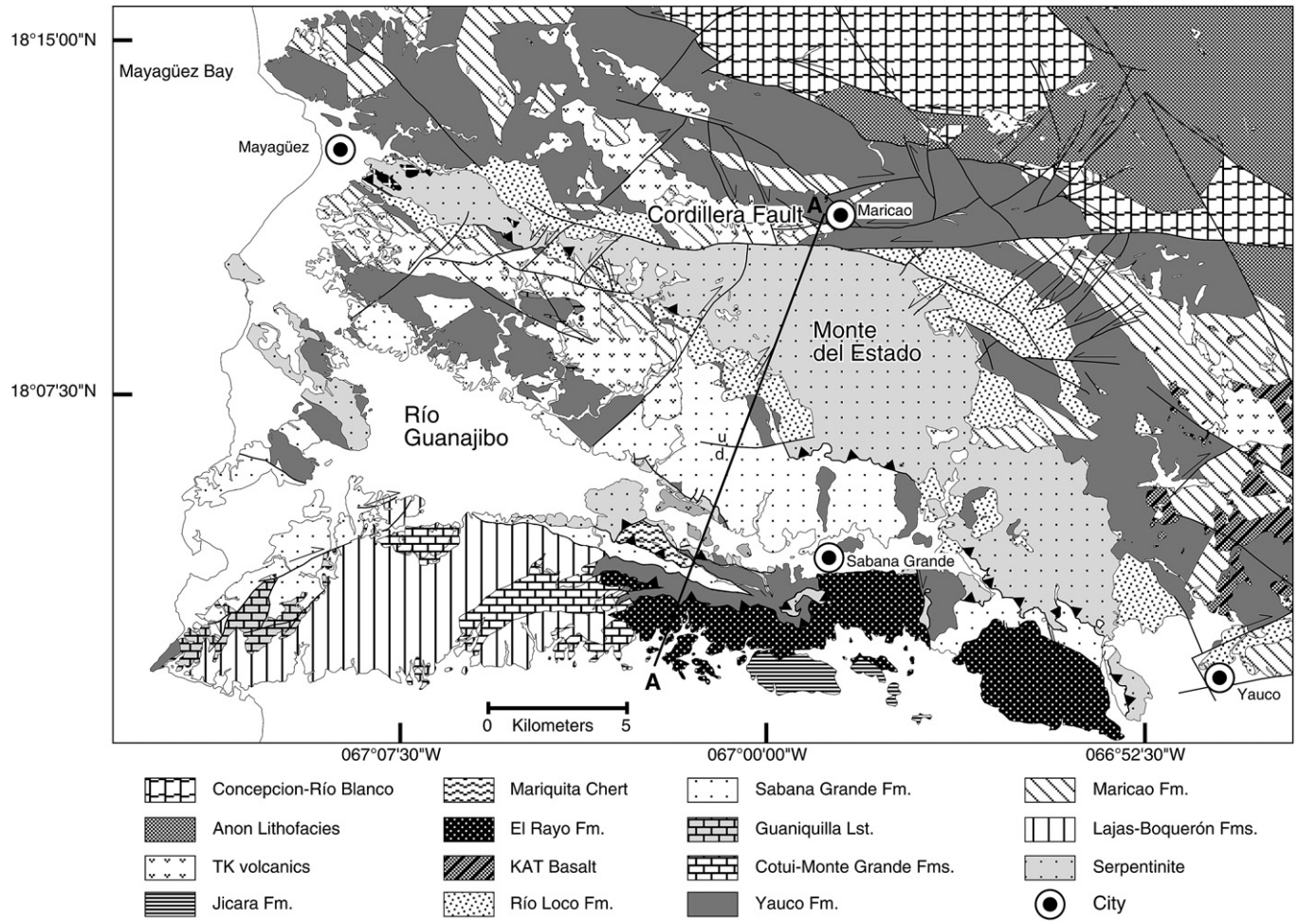

Fig. 3. Geologic map of southwestern Puerto Rico (modified from McIntyre, 1975; Krushensky and Monroe, 1978; Volckmann, 1984a, 1984b, 1984c; Curet, 1986; Martínez Colón, 2003; Llerandi Román, 2004). Heavy lines are faults with dark triangles on hanging wall of thrust fault. Lighter lines are geological contacts. Cross-section along A–A' transect is shown in Fig. 4.

into three geologically disparate blocks: northeast, central, and southwest (Fig. 2; Briggs and Akers, 1965; Glover, 1971).

The SPRFZ may have been active since the Early Cretaceous based on stratigraphic differences among Cretaceous rocks across the fault zone (Glover, 1971). Displacement along the SPRFZ is estimated to be approximately 10–22 km as recorded by displaced folds in the southern part of the fault zone (Glover, 1971; Erikson et al., 1990). Along the southwest margin of the SPRFZ younger thrust and left-lateral faulting recorded in Eocene rocks of the Cerrillos belt (Dolan et al., 1991) are attributed to transpression. Near the southern end of the fault zone, east of the town of Ponce (Fig. 2), rocks of Eocene age are thrust over Cretaceous rocks towards the northeast in association with left-lateral faulting (Glover, 1971). Erikson et al. (1990) used paleostress studies of

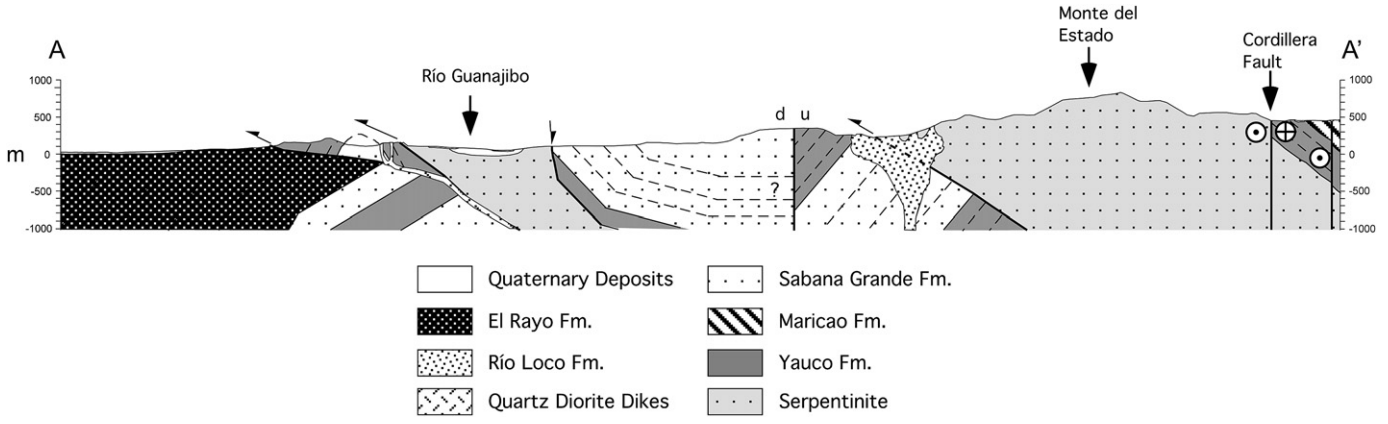

Fig. 4. Unbalanced cross-section for transect shown on Fig. 3.

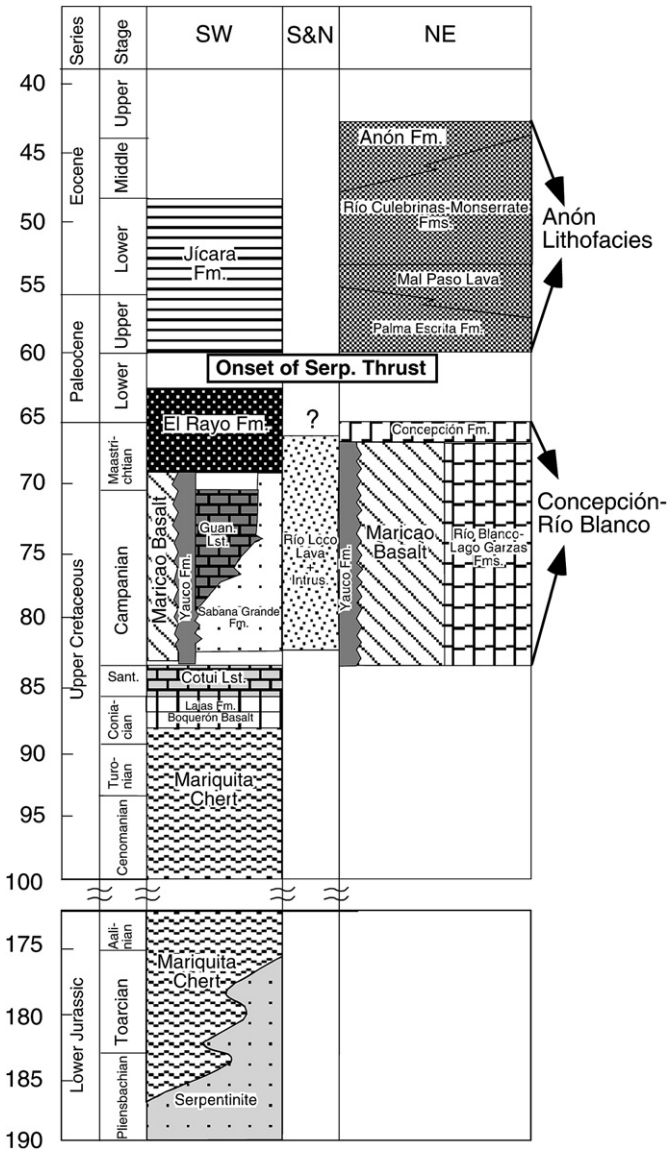

Fig. 5. Stratigraphic column for southwestern Puerto Rico, southwest and northeast of Monte del Estado (modified from Jolly et al., 1998; Santos, 1999, 2005). Guan. = Guaniquilla.

faults to suggest an asymmetric flower structure in the same region. At the northwestern limit of the SPRFZ, paleostress analysis of contractional structures in the Eocene Río Culebrinas Formation also indicates transpression with the Cerro Goden fault accommodating most of the left-lateral movement (Laó-Dávila, 2002; Mann et al., 2005).

Southwest Puerto Rico contains sedimentary, volcanic, and intrusive rocks, including Jurassic to Early Cretaceous ultramafic rocks, Cretaceous limestone, and Paleogene turbiditic rocks and limestone (Figs. 3–5). The structure of the region is generally characterized by southwest-verging folds with NW-trending fold axes, and steep faults with three different strike orientations: N45°E, N20°W, and E–W (Mattson, 1960).

2.2. Serpentinite

In southwestern Puerto Rico, serpentinite underlies about 140 km^2 (Fig. 2) and comprises three principal exposures: 1) Monte del Estado serpentinite belt, 2) Río Guanajibo serpentinite belt, and 3) Sierra Bermeja (Mattson, 1960). The northwest-trending Monte del Estado mass is the largest and northernmost serpentinite body, extending from Mayagüez Bay to the western part of the municipality of Yauco (Fig. 3). The body is widest south of the town of Maricao where it is also topographically high, reaching 900 m. In contrast, the Río Guanajibo serpentinite is a smaller, low-lying, discontinuous, belt cropping out in the Guanajibo valley with a maximum elevation of about 165 m. The westernmost Río Guanajibo exposure is at Mayagüez bay from which it extends southeast towards the town of Sabana Grande (Fig. 3). The belt comprises isolated masses including Punta Guanajibo, San Germán, and smaller bodies to the east. Sierra Bermeja, which lies south of Lajas valley, is a ridge trending east–west. Serpentinite in the Sierra Bermeja, although not conspicuous, crops out beneath more extensive chert. Amphibolite, metabasalt, and schist also occur within and around the serpentinite in this ridge.

The composition of the Río Guanajibo and Monte del Estado serpentinite is mostly chrysotile and lizardite (Hess and Otalora, 1964; Curet, 1981) that formed from ultramafic protolith comprising harzburgite, dunite, and lherzolite (Mattson, 1964; Schwartz, 1970; Curet, 1981). Fragments of amphibolite, schist, metabasalt, and chert, which are included within the serpentinite in the three belts (Schellekens, 1998), are the most abundant rock types in the Sierra Bermeja body.

The presence of serpentinite and other fragments in Sierra Bermeja led Mattson (1973) to propose that this southernmost belt is a serpentinite mélange, which was emplaced as a northward-directed (present coordinates) thrust nappe in the Early Cretaceous. The obducted body may reflect a collision that occurred in response to a change in subduction polarity from northward- to southward-directed (present coordinates; Mattson, 1973). Subsequent uplift and erosion of the serpentinite was postulated based upon the presence of serpentinite clasts at the base of Yauco and Sabana Grande formations (Mattson, 1960; McIntyre, 1975; Curet, 1986; Martínez Colón, 2003; Llerandi Román, 2004). Sedimentary and volcanic rocks accumulated upon the serpentinite during the Late Cretaceous. Mattson (1960) also proposed that the serpentinite and the Late Cretaceous rocks were folded during the Maastrichtian, with the serpentinite occupying the cores of anticlines. Mattson and Schwartz (1971) suggested that diapirism continued to move the serpentinite upwards, in some places over the Late Cretaceous rocks.

3. Serpentinite structures

Some structures within the serpentinite preserve early deformation as shown by pre-serpentinization high-temperature structures as well as structures that may have developed during serpentinization, initial uplift, and emplacement of the peridotite onto Puerto Rican volcanic units. Early formed structural and textural features based on mineral and texture formation include: 1) foliations and lineations recorded by pyroxene that formed during high-temperature flow before serpentinization, 2) kernel joints or core-and-rim fractures formed by volume increase during serpentinization (O'Hanley, 1992, 1996), and 3) textural variability of the rock (e.g. massive, phacoidal) caused by differential serpentinization and recrystallization. Tectonic stresses that were imposed upon the early template of previously formed planes may have re-activated those that are appropriately oriented, leading to formation of shear zones.

3.1. Serpentinite textures

The texture of the serpentinite may be massive, brecciated, or schistose. Color varies among orange-green, dark green–grey, reddish, and blue–green. Both color and texture may vary within

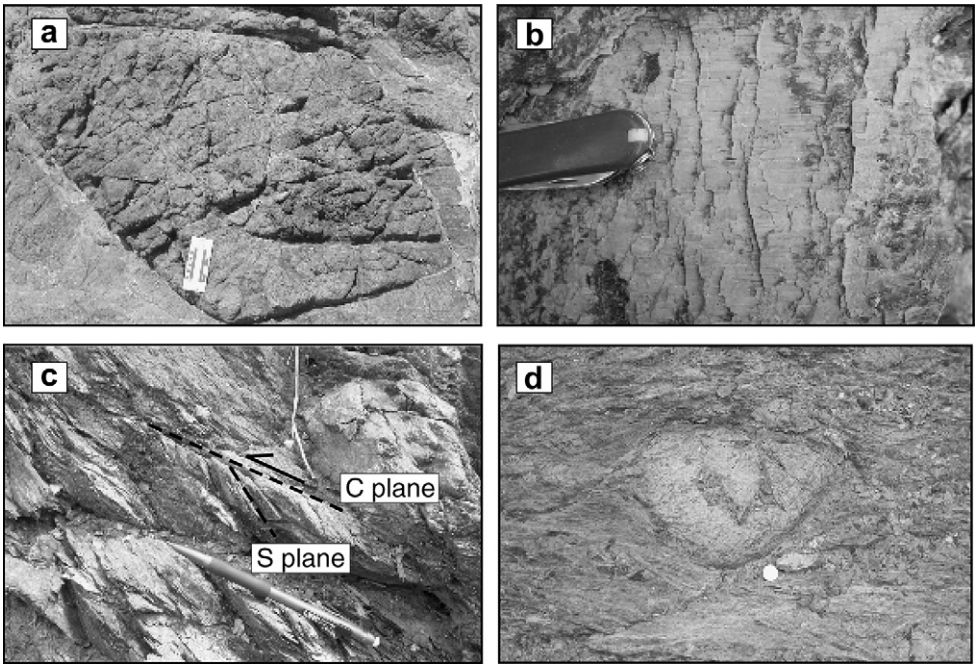

Fig. 6. Serpentinite structures: a. Fractured massive serpentinite showing early deformation joints (18°09′55″N, 067°11′06″W), b. Slickensided steps on fault plane indicating direction of slip towards the left (18°08′14″N, 066°57′22″W), c. Shear zone showing S–C fabric and slip direction (18°11′30″N, 067°08′05″W), d. Serpentinite clast within shear zone (18°04′54″N, 067°04′17″W).

a few meters in an outcrop. Core-and-rim texture (O'Hanley, 1996) is common in massive serpentinite (Fig. 6a). Good examples of core-and-rim texture are exposed at the coastal outcrops of the Río Guanajibo mass. Joints are common, especially at the interface between the core-and-rim textures, where the oldest joints formed in response to volume increase during serpentinization (O'Hanley, 1996). Spaced joints can also form a tabular texture in massive serpentinite. Massive serpentinite also may contain veins filled by oriented serpentine crystals. Some of the veins, up to 2 cm thick, are sheared and surround the serpentinized cores. Bastite crystals, up to 2 cm long, are conspicuous in massive serpentinite and commonly define foliation and lineation.

Massive blocks of resistant core serpentinite with relict bastite crystals are commonly preserved within shear zones or schistose serpentinite. Much of the massive serpentinite has polished slickensided surfaces indicating fault-slip movement along fractures

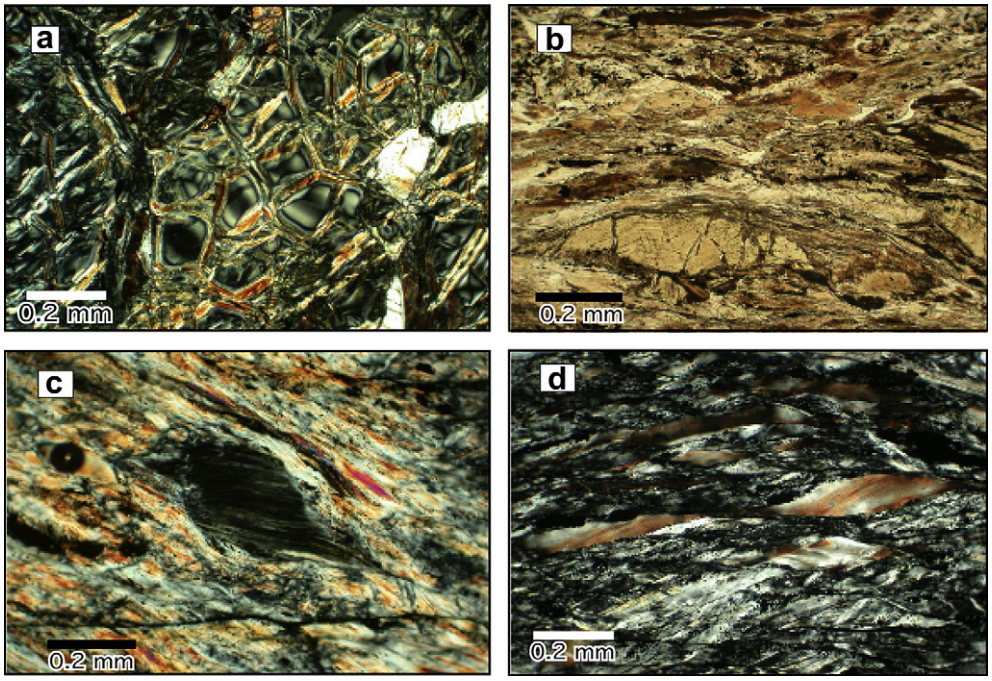

Fig. 7. Serpentinite microstructures: a. Cross-polarized light photograph of serpentinized peridotite showing mesh texture with cores surrounded by chords, b. Microphotograph of sheared serpentinite showing elongated and kinked bastite aligned with foliation, c. Bastite porphyroblast in cross-polarized light, d. S-C fabrics in serpentine under cross-polarized light.

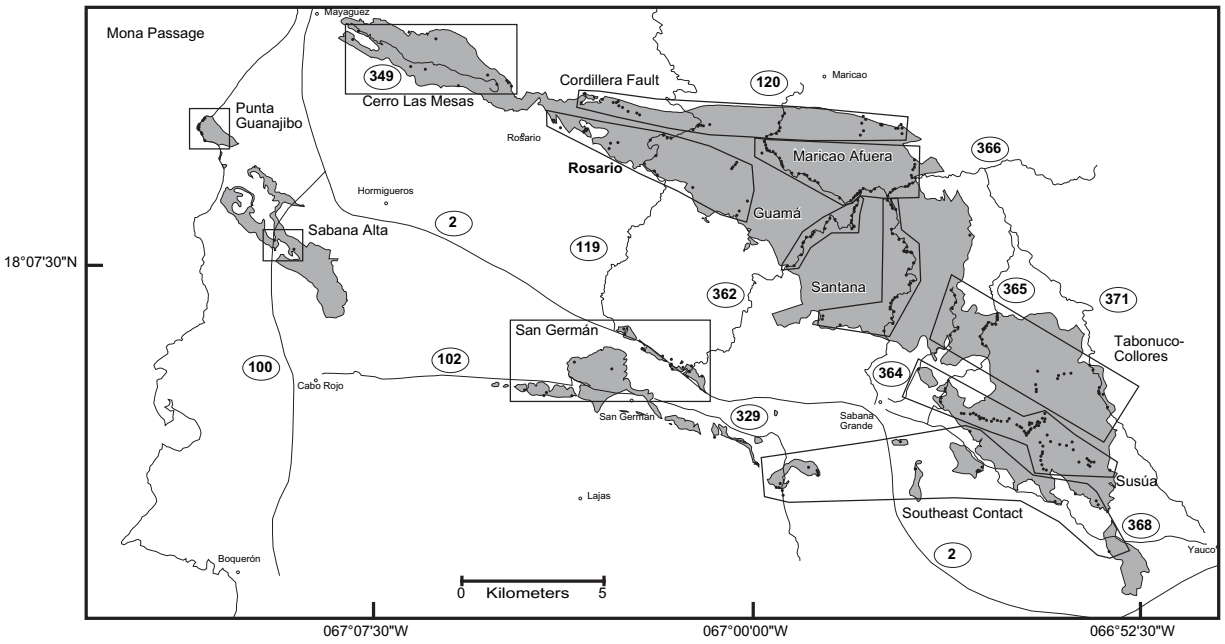

Fig. 8. Map showing domains, and data collection sites in the Monte del Estado and Río Guanajibo serpentinite. Boxes indicate area encompassed by each domain and data sites within it. Numbers inside ovals indicate road numbers. Map of serpentinite is adapted from Curet (1986), Volckmann (1984b, 1984c), McIntyre (1975), Martínez Colón (2003), and Llerandi Román (2004).

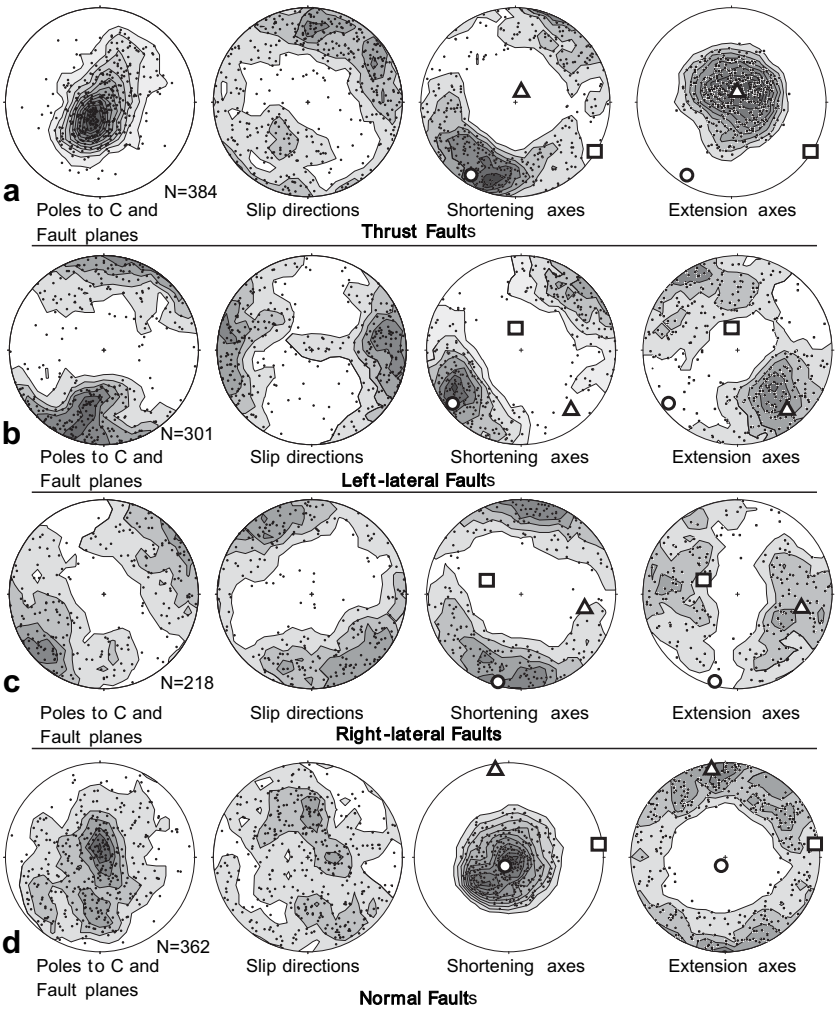

Fig. 9. Shear zone data for Monte del Estado serpentinite grouped by type. a. Thrust faults, b. Left-lateral faults, c. Right-lateral faults, d. Normal faults, Circle = maximum strain direction, square = intermediate strain direction, triangle = minimum strain direction. Kamb contours are used to display data. Contour interval = 2.0 sigma.

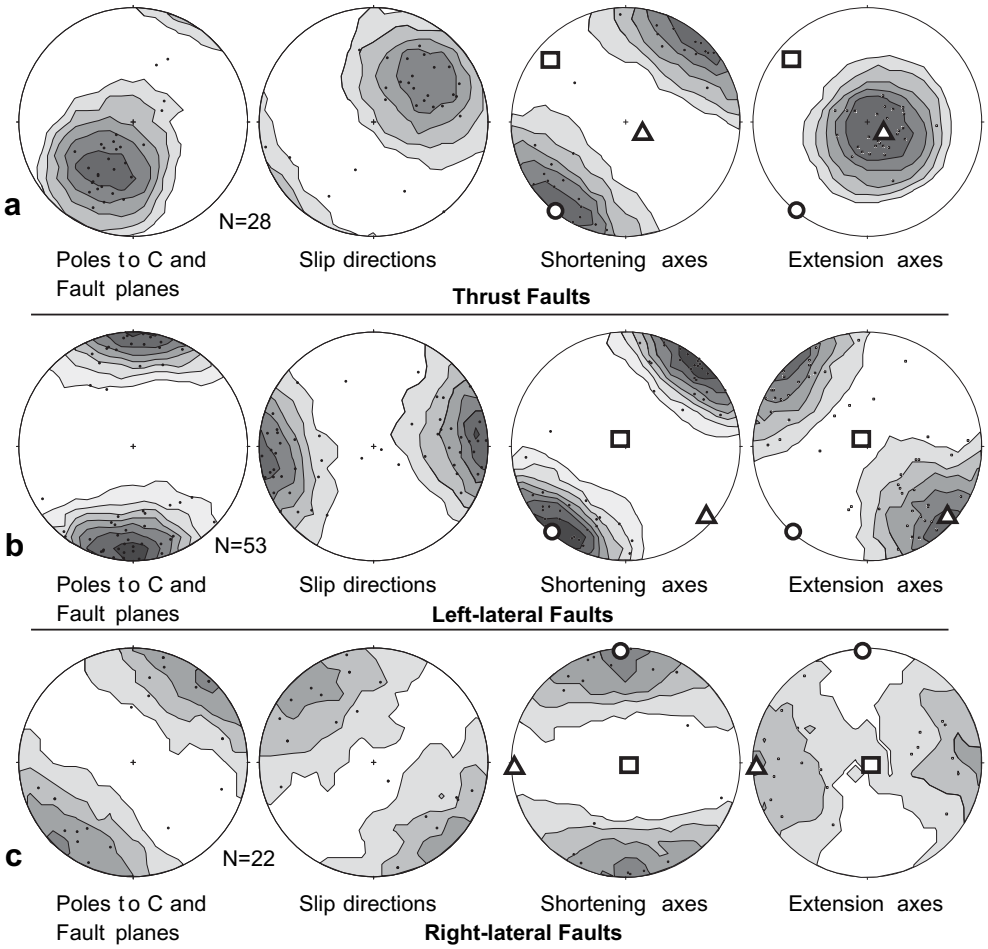

Fig. 10. Shear zone data for Río Guanajibo serpentinite grouped by type. a. Thrust faults, b. Left-lateral faults, c. Right-lateral faults, d. Normal faults. Circle = maximum strain direction, square = intermediate strain direction, triangle = minimum strain direction. Kamb contours are used to display data. Contour interval = 2.0 sigma.

(Fig. 6b). Curvilinear faults have developed commonly where slip is accommodated along connecting fractures. The abundance of these varied structural features results in a strongly deformed rock containing faults and shear zones with diverse orientations.

3.2. Serpentinite microstructures

Evidence for crystal–plastic deformation is preserved by crystals of olivine and bastite, and platy serpentine. Recrystallization of olivine is indicated by the presence of neoblasts around porphyroclasts, 120° grain boundaries, and undulose extinction. Bastite shows undulose extinction, kinking, subgrains and deformation bands. Alignment of long axes of bastite crystals defines foliation and lineation.

Serpentinized peridotite is characterized by the pseudomorphic texture in which outlines and crystals of relict olivine and pyroxene are preserved (Fig. 7a). Preexisting granuloblastic and porphyroclastic textures in olivine, and more commonly porphyroclastic pyroxene characterize the serpentinized peridotite from the study area. Platy serpentine also shows undulose extinction. Serpentinization creates mesh (Fig. 7a) and hourglass textures in the rock. In places the mesh texture is stretched and forms a ribbon texture. Overlapping mesh rims indicate serpentine recrystallization. Replacement is suggested by a change from mesh texture to interlocking texture in cores and bastite. Interlocking and rarely interpenetrating textures replace mesh texture in some of the samples indicating a transition from pseudomorphic to non-pseudomorphic textures.

Non-pseudomorphic textures and S–C fabrics that show sense of movement characterize sheared serpentinite. Of the non-pseudomorphic textures, interlocking texture is more common than interpenetrating texture. In places, elongate remnants of mesh and ribbon textures occur within foliated non-pseudomorphic serpentinite. Porphyroclastic bastites are common within foliated serpentinite (Fig. 7b).

Foliation in non-pseudomorphic serpentinite is defined by elongate bastite, blades of serpentine, and magnetite grains. The foliation commonly records folds. Foliation (S-planes) defined by aligned bladed serpentine and aligned serpentine crystals, and fractures defining C–planes form an S–C fabric that is pervasive throughout the foliated serpentinite (Fig. 7c). Elongate masses of serpentinite with interlocking texture are aligned with foliation. Serpentinite, bastite, spinel, and magnetite grains may form mantled porphyroclasts within sheared serpentinite (Fig. 7d). Individual elongate bastite grains, which show undulose extinction, may be kinked, bent, or folded (Fig. 7b).

4. Kinematic analysis

4.1. Methods

Serpentinite bodies from the Monte del Estado and Río Guanajibo belts were chosen because they are commonly well exposed and comprise large coherent masses. The orientations of planar and linear structures as well as sense of slip along faults and shear zones

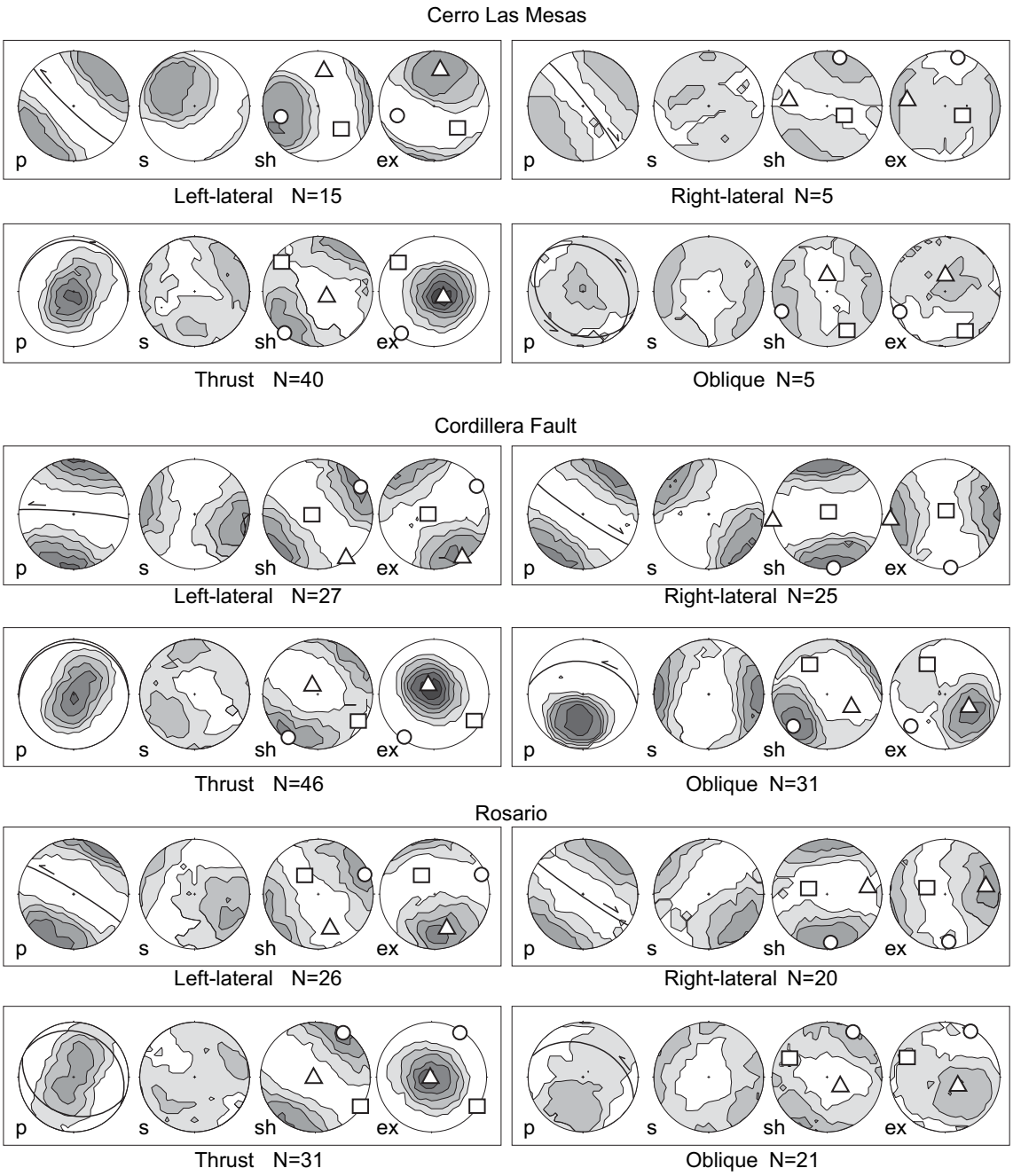

Fig. 11. Equal-area stereographic projections of structural data in the serpentinite for each domain (see Fig. 7). p = poles to C– and fault planes, s = slip directions, sh = shortening axes, ex = extension axes, Circle = maximum strain direction, square = intermediate strain direction, triangle = minimum strain direction. Contours show line concentrations. Contour interval = 2.0 sigma.

were measured from exposures along roads, rivers, quarries, cuts at construction sites, and coastal exposures. Sense of slip along faults was determined by offset of rock layers, drag folds, and steps in slickensided surfaces. In shear zones, sense of shear was determined from S–C fabric and drag folds in the serpentine foliations. The slip direction in S–C fabrics is recorded on the C–plane and is perpendicular to the intersection of the S– and C–planes (Berthé et al., 1979; Stuart-Smith, 1990). Fault-slip and shear zone data are plotted on equal-area stereographic projections and analyzed for incremental strain principal directions. Faults and shear zones are grouped and analyzed together because they cut each other and show similar orientation of strain axes.

Shortening and extension (P and T) axes are calculated for geographic domains within the serpentinite using the method from Marrett and Allmendinger (1990). Each pair of axes lies in the movement plane that contains the slip vector (e.g. striation) and the normal vector (pole to fault). The axes make angles of 45° with each of the slip and normal vectors (Marrett and Allmendinger, 1990). The orientations of shortening and extension axes are calculated from measurements in the shear plane without interpretation (Marrett and Allmendinger, 1990). Shortening and extension axes were averaged separately and contoured using Faultkin software (Marrett and Allmendinger, 1990) and the Kamb method (Kamb, 1959). The strain analysis performed in this study

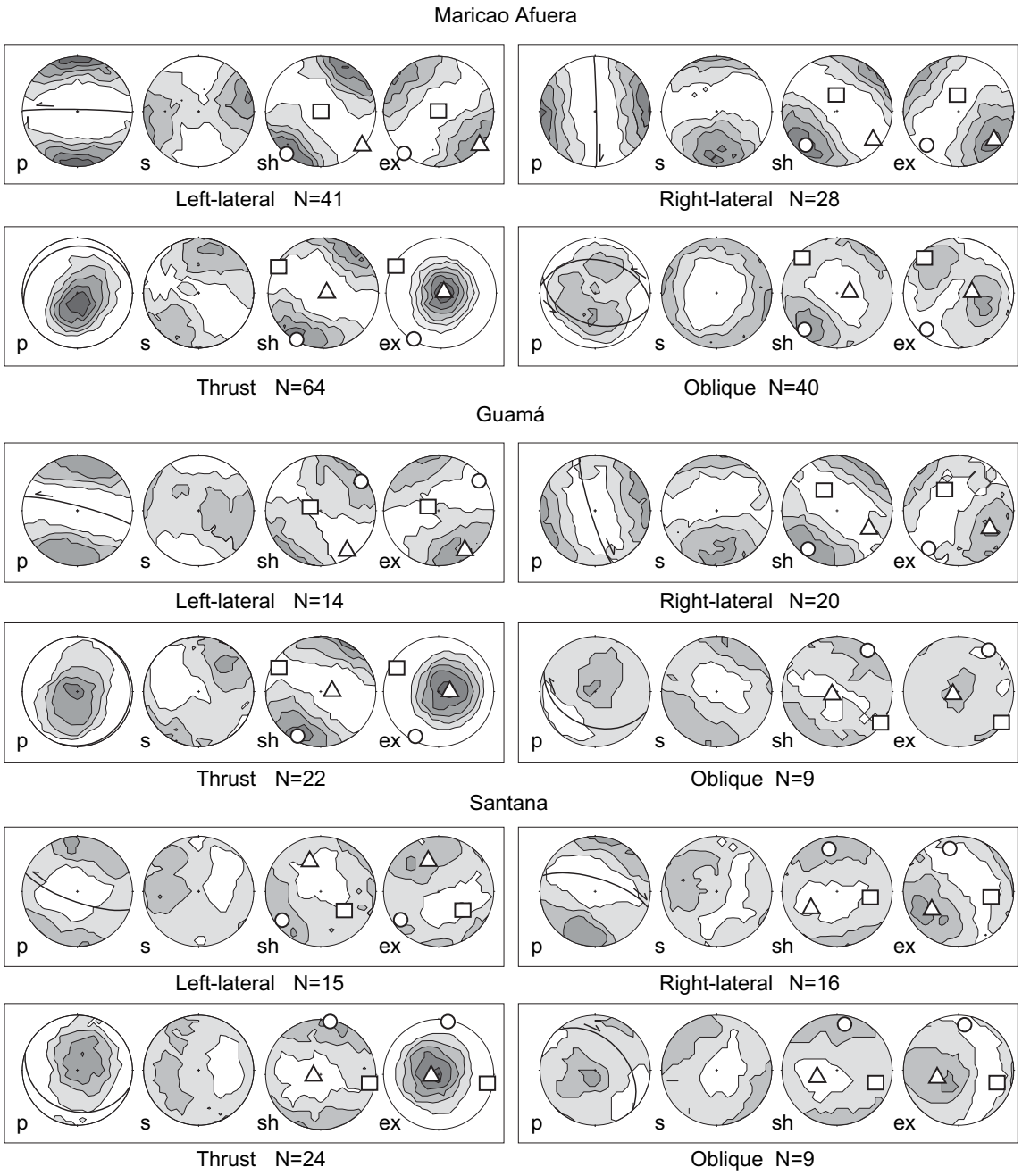

Fig. 11. (*continued*).

incorporates the following assumptions: 1) sampling is representative, 2) no post-faulting reorientation of the fault-slip directions, and 3) fault kinematics are scale-invariant (Marrett and Allmendinger, 1990).

The microrotation method (Twiss and Gefell, 1990; Twiss et al., 1991; Twiss and Unruh, 1998) is another analysis that takes into account the rotation of blocks within a rock mass based upon fault-slip analysis. The microrotation method may be useful to analyze fault-slip data in serpentinite breccia in which most blocks show slickensides with slickenlines. Such surfaces were not the emphasis of this study that focuses mainly upon thoroughgoing faults and shear zones. Most measurements are from S–C fabric rather than slickenlined surfaces. Additionally the shear planes used in the microrotation method need to be associated with a larger fault with known orientation to determine the sense of slip, which was not always the case for the faults in this study. For these reasons we chose not to use the method developed by Twiss and colleagues and use instead the method developed by Marrett and Allmendinger (1990).

4.2. Results

4.2.1. Shear zones

Conspicuous, discrete, shear zones that commonly cut the serpentinite may be developed within wider zones of folding, faulting, and foliation (Fig. 6b–d). S–C planes that help to distinguish these shear zones are the most common shear structures in the serpentinite (Fig. 6c). Of 1846 shear planes, 1422 planes had reliable sense

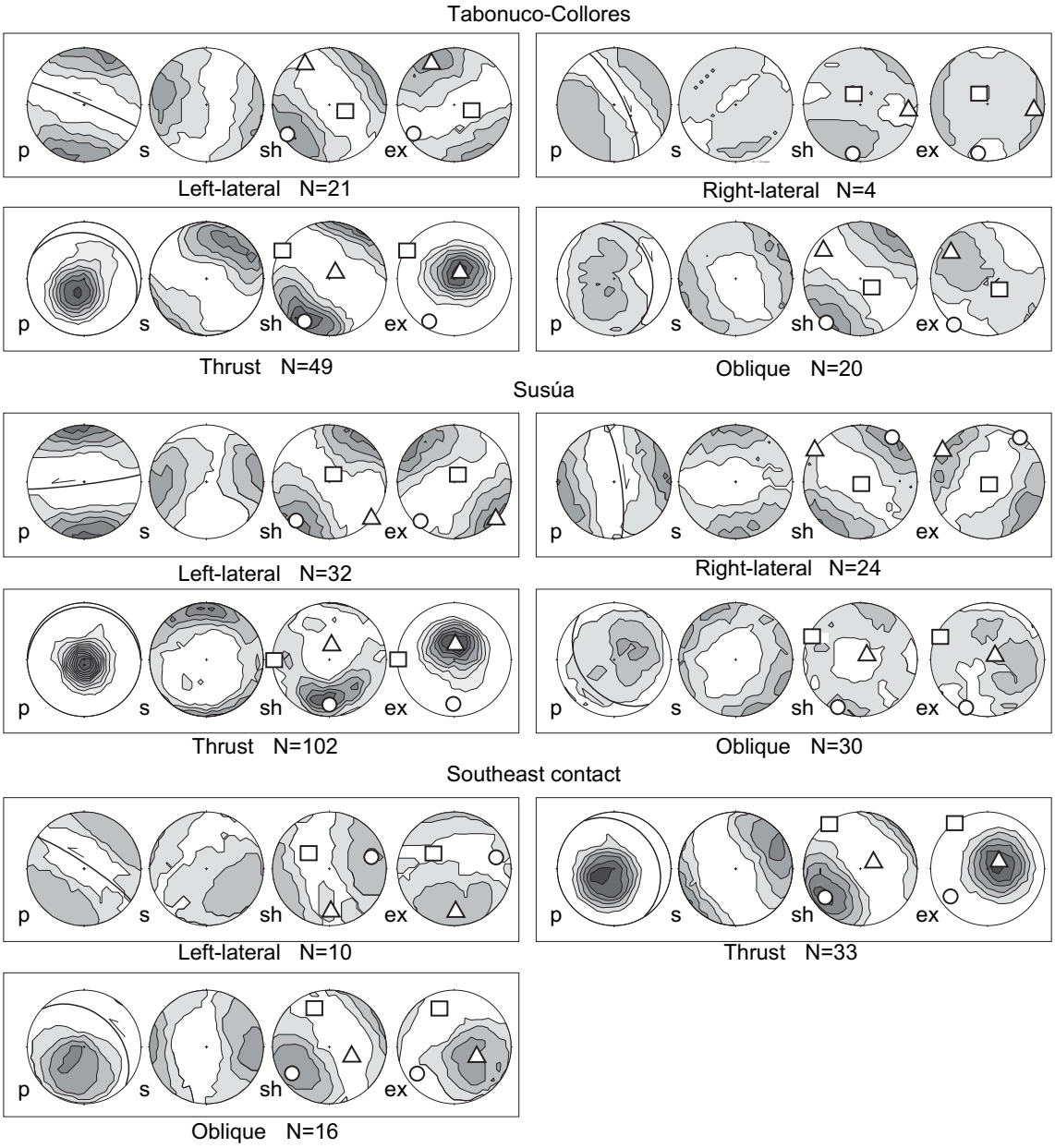

Fig. 11. (*continued*).

of slip indicators. The measurements, collected from outcrops at more than 300 stations, are grouped into domains (Fig. 8) based on spatial relationships such as: 1) isolated bodies (e.g. Cerro Las Mesas domain), 2) proximity to major structures or contacts (e.g. Cordillera Fault and Rosario domains), and 3) data collected along a road (e.g. Santana domain). Strain results are presented for every domain as opposed to every station because of the difficulty of displaying the data for more than 300 stations. Moreover, presentation of data as shear plane type (thrust, strike-slip, and oblique) yields a more robust strain characterization for the study area. Results are shown in Figs. 9–11 and in Table 1.

4.2.1.1. Thrust faults. The most common planar structures are shear zones with thrust or reverse sense of movement. Most thrust faults strike NW–SE, have a low dip angle ($<30^\circ$), and show top towards S or SW. However, within Cerro Las Mesas, Cordillera Fault, Maricao Afuera, and Susúa domains strikes are E–W. In the Rosario and Sabana Alta domains the faults strike ESE (Fig. 11). Slip lines plunge NE or N (Fig. 9a) in all domains.

4.2.1.2. Left-lateral faults. Left-lateral shear zones are the most numerous strike-slip shear zones in the study area (Figs. 9b and 10b). Most of these structures strike WNW–ESE and have dips greater than 60°. Oblique shear zones that strike E–W and dip 30°–60° to the N or S are also common. Northwest–southeast striking left-lateral shear zones characterize the structure of Cerro Las Mesas, Rosario, and Southeast contact domains (Fig. 11). Most left-lateral shear zones strike E–W within the Punta Guanajibo, San Germán, Maricao Afuera, and Susúa domains. Whereas most slip lines trend E and W, variations in trend exist among domains. Slip lines within fault zones in Cerro Las Mesas, Rosario, and Santana domains trend NW and SE. In Maricao, Afuera, and Guamá they trend E and W. However, they trend ESE and WNW in the Cordillera Fault domain, and WSW and ENE in the Susúa domain.

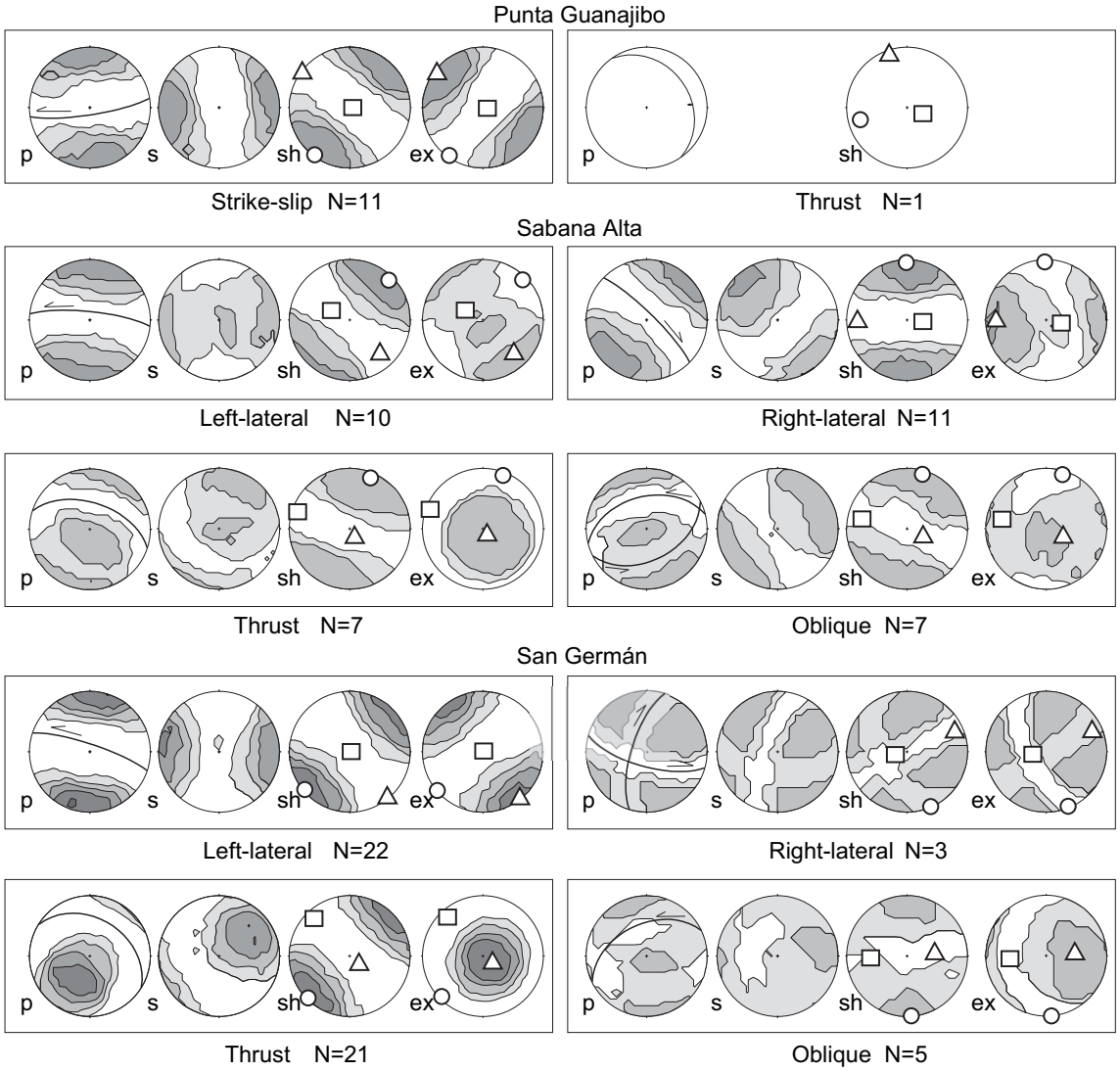

Fig. 11. (*continued*).

4.2.1.3. Right-lateral faults. Most right-lateral faults are steep and strike NW–SE (Figs. 9c and 10c). Less common oblique right-lateral faults also strike NW–SE. Some of these orientations are similar to left-lateral shear zones, however, cross-cutting relationships indicate that right-lateral faults may be older. Northerly striking right-lateral shear zones crop out within Maricao Afuera; within the Punta Guanajibo, Guamá, Tabonuco–Collores, and Susúa domains strikes are NNW–SSE. Within the San Germán domain right-lateral faults strike E–W (Fig. 11). Most slip indicators trend SE or SSW although slip lines trend north in the Maricao Afuera, Guamá, Tabonuco–Collores, Susúa, and Punta Guanajibo domains.

4.2.1.4. Normal faults. Shear zones with normal sense movement are conspicuous and occur in all domains. Most have shallow dips and strike E–W. A set has slip lineations that trend NNW and SSE, and a smaller group of shear zones shows easterly slip direction (Fig. 9d). Normal shear zones are grouped and discussed together because they cut thrust and strike-slip faults and therefore are believed to be younger than the shortening structures.

4.2.2. Age of structures

Relative timing of structures within the serpentinite is difficult to establish because structures with different orientations are common and because many faults have been re-activated. In general left-lateral shear zones cut right-lateral and thrust shear zones. Thrust and right-lateral shear zones cut each other, and right-lateral shear zones may cut left-lateral shear zones. These relationships suggest that many strike-slip faults and thrusts are coeval, and that shear zones may have been re-activated.

Grouping structures based on the orientation of the strain axes, dip of shear planes, and shortening orientation (N–S, NE–SW, E–W, NW–SE) yields insight into probable relative ages (Fig. 12). For N–S shortening, maximum strain axes with azimuths of 45° or less from the N–S direction are grouped. The relation of strike and dip of each structure to the orientation of the minimum strain axis may be used to distinguish groups of strike-slip, oblique, and thrust faults. Minimum strain axes with plunges greater than 60° are interpreted as thrust faults. Structures with dips ranging from 30° to 60° and minimum strain axes plunging less than 60° are grouped with faults recording oblique slip. Structures with both minimum and maximum strain axes plunging less than 60° and dips greater than 60° are grouped with strike-slip faults. A similar analysis was performed for faults with shortening directions of the NE–SW, E–W, and NW–SE.

Despite the complexity stemming from re-activation of many faults, the ages of the fault groups are compatible with the generally

Table 1
Strain axes for geographic domains throughout the serpentinite. LL = left-lateral; RL = right-lateral; O = oblique; T = thrust. Axes orientations presented as azimuth/plunge.

Domain	Type	Axis 1 (shortening)	Axis 2 (intermediate)	Axis 3 (extension)	*N*
Cerro Las Mesas	LL	256/32	133/41	033/10	15
	RL	014/008	117/59	280/30	5
	O	246/11	152/22	001/65	5
	T	219/04	310/16	116/74	40
Cordillera Fault	LL	056/06	278/82	147/06	27
	RL	173/04	021/86	263/02	25
	O	227/16	329/37	118/48	31
	T	215/06	123/12	330/77	46
Rosario	LL	067/009	324/55	162/34	26
	RL	176/13	291/60	80/26	20
	O	029/04	297/25	126/65	21
	T	033/03	123/01	234/87	31
Maricao Afuera	LL	219/02	347/87	129/03	41
	RL	223/17	353/64	127/19	28
	O	223/13	316/12	087/72	40
	T	212/03	302/02	065/86	54
Guamá	LL	053/09	293/73	146/14	14
	RL	218/14	327/54	119/33	20
	O	036/07	126/04	243/82	9
	T	208/10	300/14	084/72	22
Santana	LL	234/16	129/43	339/43	15
	RL	349/22	098/39	237/43	16
	O	009/16	107/27	252/58	9
	T	010/01	100/09	272/81	24
Tabonuco-Collores	LL	236/13	112/68	330/18	21
	RL	190/14	325/71	097/13	4
	O	217/00	127/70	308/20	20
	T	211/12	302/03	045/77	49
Susúa	LL	221/12	029/78	131/03	32
	RL	035/001	140/87	305/03	24
	O	205/09	296/06	061/79	30
	T	181/22	271/01	004/68	102
Southeast contact	LL	074/24	309/53	177/27	10
	O	236/22	338/28	113/54	16
	T	234/21	325/05	067/68	33
Punta Guanajibo	SS	217/04	084/85	307/04	13
Sabana Alta	LL	044/06	303/62	138/27	10
	RL	359/03	096/70	268/20	11
	O	016/05	284/24	117/65	7
	T	021/06	291/08	148/80	7
San Germán	LL	230/03	020/87	140/01	22
	RL	158/03	258/74	067/15	3
	O	176/01	266/39	085/51	5
	T	226/04	317/14	121/75	21

observed cross-cutting relations. Shear zones compatible with N–S and NE–SW shortening directions cut each other. Shear zones compatible with E–W shortening commonly cut shear zones compatible with NE–SW shortening, and also to a lesser extent cut shear zones compatible with N–S shortening. Shear zones compatible with E–W shortening are cut by few other shear zones and may be relatively young. Shear zones compatible with NW–SE shortening cut all other shear zones the least. Contractional structures that are compatible with a NE–SW and N–S shortening directions are cut the most by other structures. These cross-cutting relationships suggest that shear zones compatible to shortening directions of N–S and NE–SW are older whereas structures formed during E–W shortening are younger. Moreover, some NW–SE striking left-lateral shear zones seem to cut along preexisting NW–SE striking right-lateral shear zones as indicated by re-activated shear planes.

Absolute ages of deformations are difficult to establish because of the lack of isotopic ages. However, at the southern contact of Monte del Estado, serpentinite is thrust over steeply dipping late Maastrichtian–Paleocene limestone and volcanic rocks of El Rayo Formation (Slowdowski, 1956; Llerandi Román, 2004). This relationship indicates that contractional deformation of the serpentinite occurred during or after late Maastrichtian–Paleocene. Furthermore, the steeply tilted beds of the Paleocene–Eocene Jicara Formation may be rotated due to this deformation.

Normal faults generally cut strike-slip and thrust shear zones and therefore are believed to be young. However, because normal shear zones that are compatible with the contractional strain regimes (i.e. perpendicular to thrust shear zones) may have formed at the same time as the shortening structures, relatively old normal faults are not precluded.

Faults and shear zones within the serpentinite cut each other, indicating similar age and conditions for their development.

4.2.3. Kinematic significance of shear zones

Conspicuous southwesterly directed shortening is recorded by some structures in all domains although variability in the shortening directions is shown locally. Kinematic axes for shear zones grouped by sense of displacement are shown in Fig. 9. Thrust and right-lateral shear zones show the most variability in shortening direction, whereas left-lateral strike-slip faults define tight clusters of shortening axes. Extension axes derived from analysis of strike-slip shear zones show intermediate strain axes that plunge $\sim 45^{\circ}$ indicating the presence of oblique shear zones. Extension axes from the normal shear zones of the Monte del Estado distinguish two groups with NE–SW and NNW–SSE extension directions (Fig. 9d).

Shortening directions determined from thrust and strike-slip shear zones cutting the serpentinite in Monte del Estado generally trend SSW to WSW. Conjugate and strain compatible structures can be divided into three main groups based on shortening directions (Fig. 12): 1) NW–SE striking right-lateral faults, fewer NE–SW striking left-lateral faults, and an E–W striking thrust shear zones that record N–S shortening; 2) the largest group of structures that records NE–SW shortening and consists of E–W mostly oblique left-lateral faults, N–S right-lateral shear zones, and NW–SE striking thrust shear zones; 3) NW–SE striking left-lateral shear zones comprise a third fault group that records E–W shortening. Rare shear zones accommodate NW–SE shortening. Slickenlines on C–planes may have the same kinematic direction as indicated by the intersection of S–C planes. In addition, many faults have different sets with different orientations of slickenside striations indicating multiple fault movements.

Fig. 13 presents a summary of maximum horizontal shortening direction by domain that incorporates the strain compatibility of structures. Structures are grouped within a single domain according to the orientation of the principal strain axis as shown in Fig. 11. Structures that had sub-vertical intermediate and minimum strain axes are grouped together if the structures had similar incremental shortening orientations. The structures are separated into two groups if the incremental shortening axes show different orientations. The maximum horizontal shortening directions from these groups are shown as arrows in Fig. 13.

Strain axes within the Monte del Estado body generally trend NE and SW. In the Cerro Las Mesas domain, the general shortening direction of left-lateral and thrust shear zones is WSW (Fig. 11). Here, thrust faults commonly show SW-directed shortening. At the northern boundary of Monte del Estado, near the Cordillera fault (Cordillera Fault and Rosario domains), strike-slip faults show two maxima indicating southward- as well as southwestward-trending shortening. Thrust faults in the Cordillera Fault domain also show

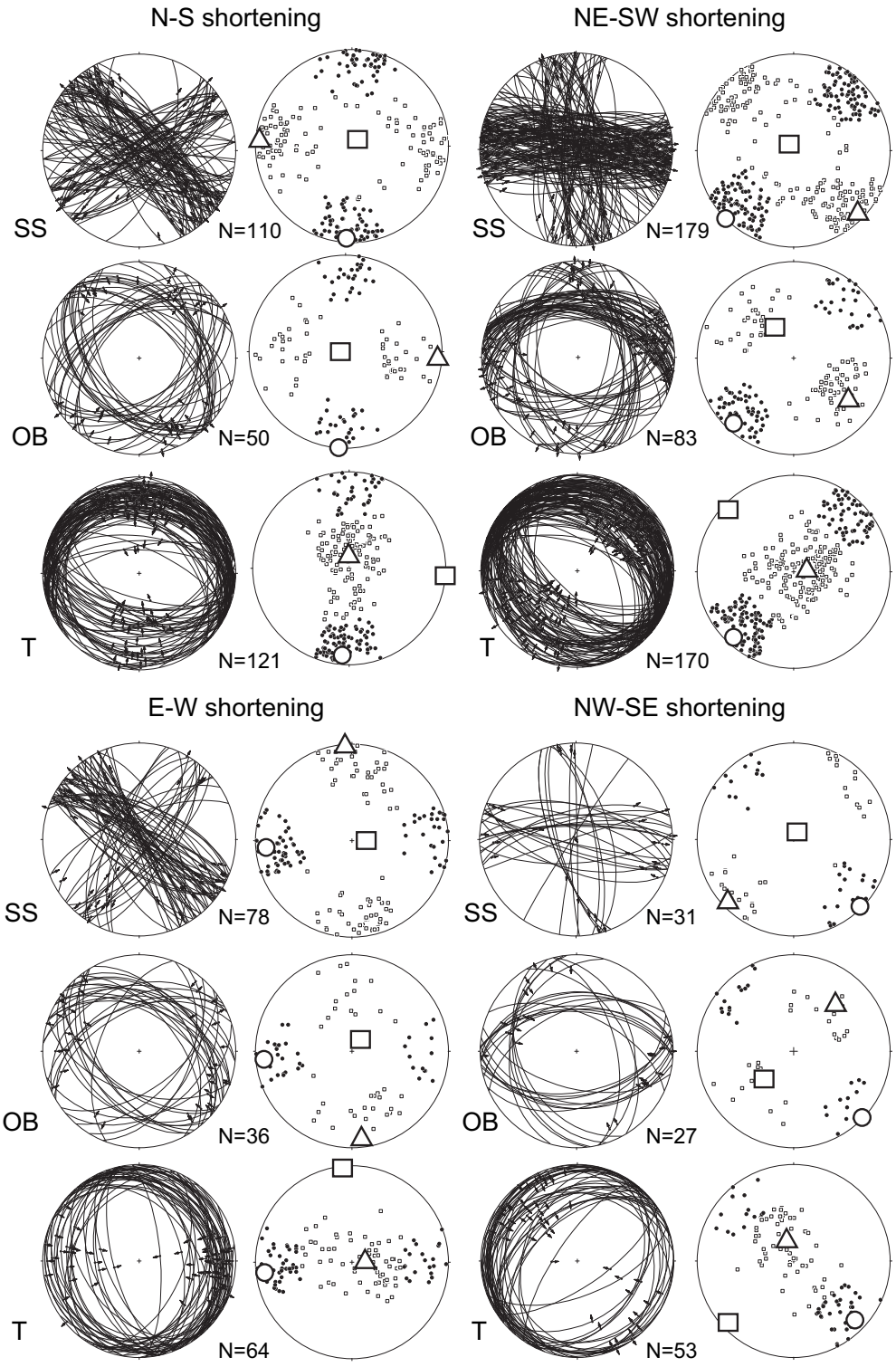

Fig. 12. Shear zone slip data for Monte del Estado and Río Guanajibo areas grouped by shortening direction. ss = strike-slip, ob = oblique, t = thrust fault, closed circles = shortening axes, open squares = extension axes, Circle = maximum strain direction, square = intermediate strain direction, triangle = minimum strain direction.

two maxima. The Santana domain shows broader and less coherent maxima compatible with SE–SW and NE–NW shortening. Thrust faults within the Susúa domain define maxima indicating contraction along S to SE directions.

Strain axes in the Río Guanajibo body are similar to those in Monte del Estado, although the directions vary less than the larger body (Fig. 10). SW-trending shortening is common throughout the mass. Strike-slip structures dominate in the coastal area at Punta Guanajibo and locally along the southern margin of the mass. Thrust shear zones dominate in other areas (Fig. 11). A south–southwesterly average shortening direction is preserved near the Sabana Alta area.

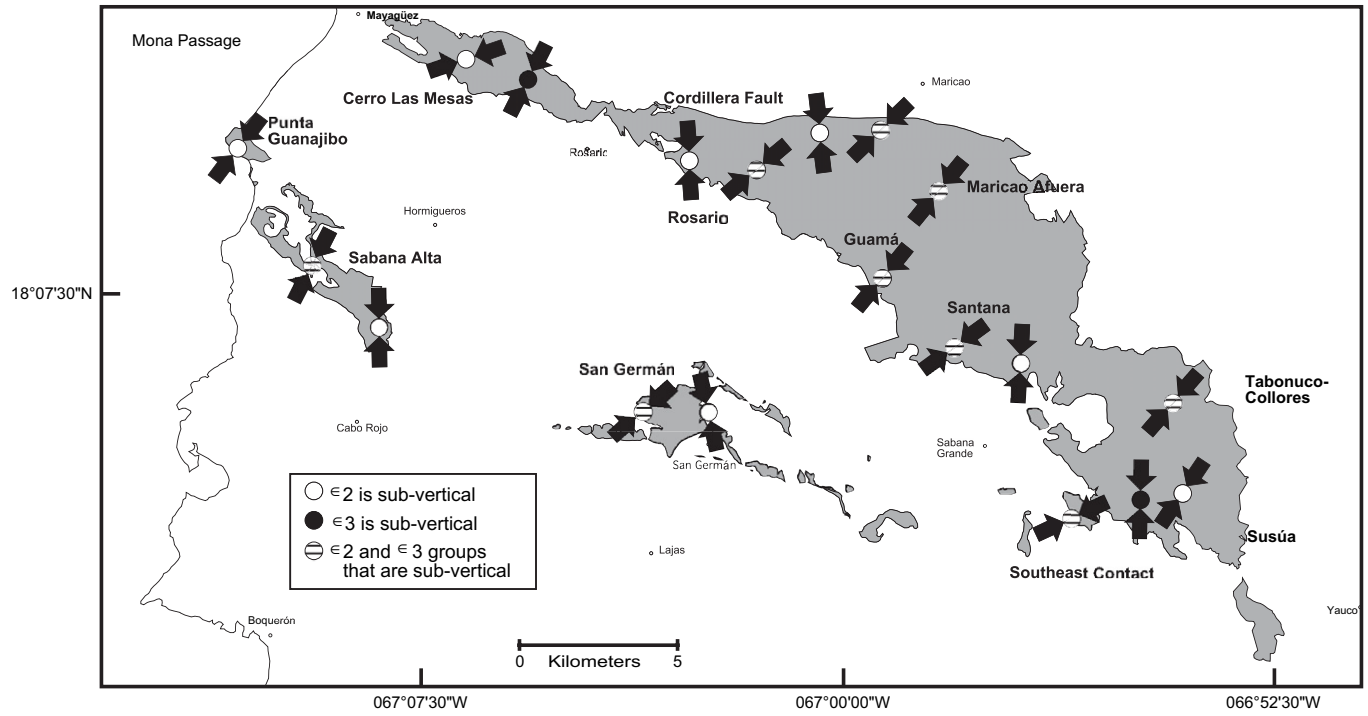

Fig. 13. Map showing strain pattern in the Monte del Estado and Río Guanajibo serpentinite. Arrows indicate maximum horizontal shortening direction. Open circles where intermediate strain axes are sub-vertical, closed circles where minimum strain axes are sub-vertical, and circles with horizontal line pattern where maximum shortening strain axes of strike-slip and thrust faults are compatible. Map of serpentinite is adapted from Curet (1986), Volckmann (1984b; 1984c), McIntyre (1975), Martínez Colón (2003), and Llerandi Román (2004).

5. Discussion

5.1. Deformation events

Kinematic analysis of contractional structures in serpentinite reveals that the oldest deformations are related to N- and NE-trending maximum strain, and that a weak younger deformation is related to an E-trending maximum strain. One possibility is that early contraction began with N–S shortening, followed by initiation of NE–SW shortening, and finally the shortening direction changed to an E–W direction (Fig. 14). The numbers of thrust and strike-slip faults associated with N- and NE-trending maximum strains are about equal. The group of shear planes of the youngest E-directed contractional deformation has about the same amount of thrust and strike-slip faults, however northwest-striking left-lateral strike-slip faults dominate.

Shear planes compatible with NW–SE shortening are few compared to other groups and their cross-cutting relationships are not clear. One possibility is that shear planes from this group are older than other fault groups and may have been rotated from shear planes originally compatible with the N shortening direction by tectonic rotation along the plate boundary. These faults do not constitute a majority in any of the geographic domains (Fig. 11), the group contains the fewest shear planes, and cross-cutting relationships are uncertain. Thus, they will be treated as rotated from other groups and will not be discussed further.

Counterclockwise rotation of southwest Puerto Rico (van Fossen et al., 1989) may account for some of the variability in shear zone orientation. Older structures may have rotated more than younger ones and there may have been rotation of faulted blocks within the serpentinite that may be responsible for the orientation difference.

Late Eocene–Early Oligocene contractional and strike-slip structures in Eocene turbidites and volcanic rocks of the Cerrillos belt are similar in orientation to structures recorded in the serpentinite. In the northern Cerrillos belt strain is partitioned between N–S and NE–SW shortening directions (Fig. 15a, b, and c; Laó-Dávila, 2002), while in the southern part shortening is NNE–SSW to ESE–WNW (Fig. 15 d and e; Erikson et al., 1990). Left-lateral faults in the southern Cerrillos belt record strain with orientation similar to the younger E-directed deformation in the serpentinite and they may be related. Older N- and NE-directed deformations in the serpentinite are compatible with the N- and NNE-directed deformations in the northern and southern Cerrillos belt because shear planes and strain axes have similar orientations. The similarity suggests that the N-, NE- and E-trending strains recorded in the serpentinite could be correlated with the tectonic events recorded by the Eocene rocks.

Thrust faults with oblique motion and strike-slip faulting characteristic of transpression are evident in the structures of the Cerrillos Belt and in the Monte del Estado and Río Guanajibo serpentinite. Thus, we suggest that transpression related to NE-trending strain documented for the Eocene rocks of the Cerrillos belt extended all throughout southwestern Puerto Rico and was a major factor in the deformation of the serpentinite. It is mostly expressed by E–W striking left-lateral shear zones and NW–SE thrusts. However, the serpentinite thrust over the late Maastrichtian–Paleocene El Rayo formation suggests that contractional deformation may have begun in the Paleocene and continued on to the late Eocene–early Oligocene.

The SW-directed thrust faults of the serpentinite contrast with the view that serpentinite deformation was related to diapirism (Mattson, 1960; Mattson and Schwartz, 1971; Volckmann, 1984b, 1984c; Jolly et al., 1998b). Thrust faults with slickenlines recording motion oblique to strike and strike-slip faults indicate a transpressional tectonic regime as opposed to an extensional tectonic regime favorable for diapirism.

The youngest deformation recorded by serpentinite consists of E–W striking normal faults related to N–S extension. However, the

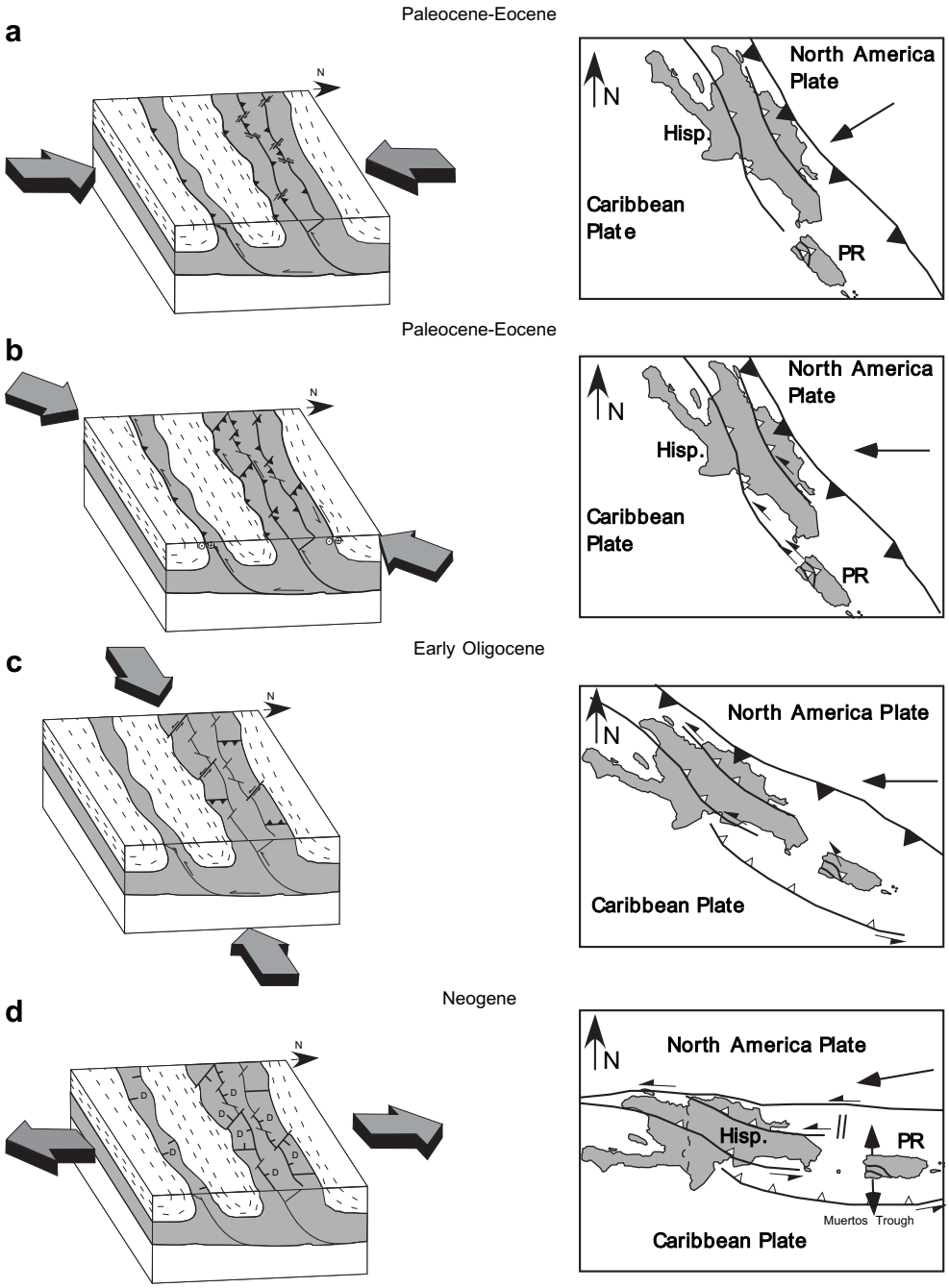

Fig. 14. Strain development in the Monte del Estado and Río Guanajibo serpentinite and plate tectonic scenario. Large arrows indicate maximum horizontal strain direction. a. North–South shortening, b. Northeast–Southwest shortening, c. East–West shortening, and d. North–South extension. Heavy lines indicate active structures. Counterclockwise rotation of Greater Antilles is based on paleomagnetic data (Reid et al., 1991; van Fossen et al., 1989).

extension is post emplacement and correlates with Miocene–Pliocene extension that occurred throughout western Puerto Rico (Laó-Dávila, 2002; Mann et al., 2005).

5.2. Regional tectonic setting

Deformational events in Puerto Rico correlate with tectonic events along the Caribbean–North American plate boundary. Three collisional events between Late Cretaceous to present are commonly recognized in the northeastern Caribbean. First, 90–74 Ma transpression in northwestern Cordillera Central of Hispaniola (Escuder-Viruete et al., 2006). Second, a collision of the Caribbean Plate with Caribeana in the latest Cretaceous to earliest Paleocene (García-Casco et al., 2008). And third, the collision of the Caribbean plate with the Bahamas bank of the North American plate during Late Paleocene to early Late Eocene (Cobiella-Reguera, 2005; Bourdon, 1985; Joyce, 1991). Paleocene–Eocene deformation of serpentinite of southwestern Puerto Rico, consisting mostly of E–W striking thrust faults and NW-striking right-lateral faults, may be related the collision of the Caribbean plate with the Bahamas bank of the North American plate. After the collision of Cuba, left-lateral shearing accommodated by NW-striking faults laterally separated the Greater

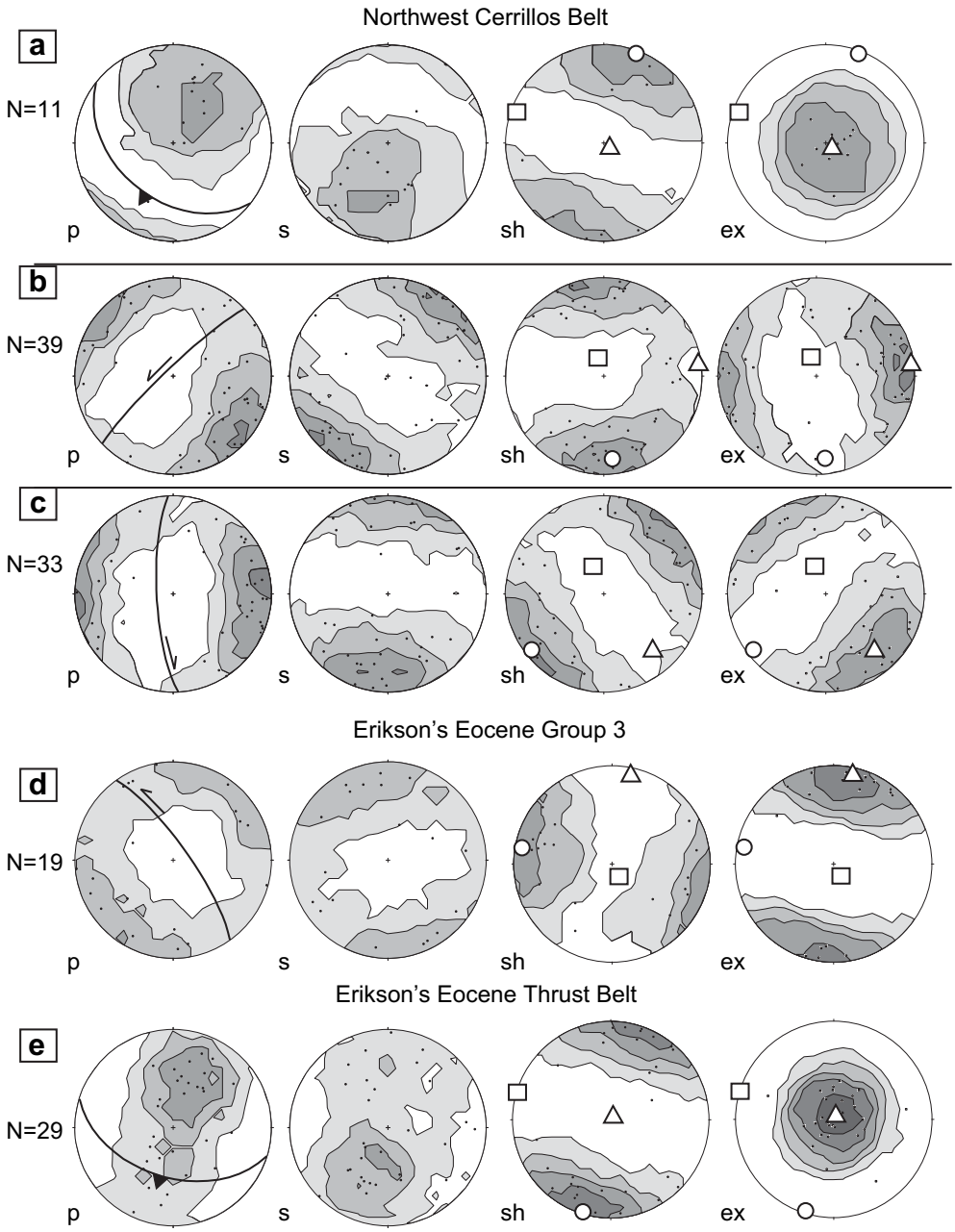

Fig. 15. Equal-area stereographic projections of structural data in Eocene rocks of the Cerrillos belt from Laó-Dávila (2002) and Erikson et al. (1990). a. Thrust faults, b. Left-lateral faults, c. Right-lateral faults, d. Left-lateral faults in the south, e. Thrust faults in the south p = poles to C– and fault planes, s = slip directions, sh = shortening axes, ex = extension axes, Circle = maximum strain direction, square = intermediate strain direction, triangle = minimum strain direction. Contours show line concentrations. Contour interval = 2.0 sigma.

Antilles. During the strike-slip faulting contraction related to transpression resulted in development of thrust faults along which hanging wall rocks were carried southwestward.

Fold and thrust belts in eastern Hispaniola may be related to the same deformational events described from the serpentinite and Cerrillos Belt in Puerto Rico. The Peralta Belt is characterized by thrust and folds formed by transpression from the Eocene to the present (Hernaiz-Huerta and Pérez-Estaún, 2002). The deformation from the Cordillera Oriental is characterized by NE-directed contraction in latest Cretaceous followed by transpression in the Eocene to present (García-Senz et al., 2007).

Anticlockwise rotation of ~45° since the Eocene and ~22° since the Miocene of Puerto Rico about a vertical axis in response to reorganization along the plate boundary from a more orthogonal to oblique subduction is postulated by van Fossen et al. (1989) and by Reid et al. (1991; Fig. 14). East trending maximum strain occurred as the last early Oligocene expression of transpression dominated by NW-trending left-lateral faults and accompanied by thrust faults. Contractional deformation ceased in Puerto Rico in mid Oligocene and the younger deformation is characterized by N–S extension in the Neogene (Laó-Dávila, 2002).

6. Conclusions

Shear zones and faults recorded by the Monte del Estado and Río Guanajibo serpentinite masses in southwestern Puerto Rico include 1) NW-striking right-lateral faults and E-striking thrust faults, 2) NW–SE striking thrust faults and E–W striking left-lateral shear

zones, and 3) a young group comprising N-striking thrust faults and NW-striking left-lateral faults. The N-trending shortening of the first group is probably the oldest; as suggested by re-activation of many E–W shear planes. The shear planes from the second group suggest deformation within a transpressional regime because of the combination of both oblique thrust faults and strike-slip faults. During development of this event the trend of the principal shortening direction was southwest as was the direction of transport. Later shortening became more westerly. Involvement of Eocene rocks indicates that the contractional and related strike-slip faults are late Eocene. Serpentinite lastly records Neogene N–S extension that is manifest throughout western Puerto Rico.

Evidence for diapirism is not evident in the structures recorded by serpentinite. Further, thrust faults, which dip NNE in southwestern Puerto Rico, show southwest-directed transport that differs from transport recorded in other serpentinite masses in the northern Caribbean. For example, some Cuban serpentinite masses, and Loma Caribe serpentinite in central Hispaniola were thrust northward in Early Tertiary.

Acknowledgements

This research was supported by grants from Exxon-Mobil and the Geological Society of America Graduate Student Grant. The Leighton Scholarship at the University of Pittsburgh also provided funds. Thanks to Edward Lidiak, James Joyce, Hernán Santos Mercado, Johannes Schellekens, Grenville Draper, Wayne Jolly and Pablo Llerandi Román for discussions and suggestions. Reynard Rohena provided fieldwork assistance. We are grateful to Wetsy Cordero and Adrián Muñiz of the Departamento de Recursos Naturales y Ambientales for assistance while working in the Susúa and Monte del Estado forests. We are grateful to Steven Wojtal and Paul Mann for careful reviews of the manuscript.

References

Andreani, M., Boullier, A.-M., Gratier, J.-P., 2005. Development of schistosity by dissolution–crystallization in a Californian serpentinite gouge. Journal of Structural Geology 27, 2256–2267.

Auzende, A.-L., Guillot, S., Devouard, B., Baronnet, A., 2006. Serpentinites in an Alpine convergent setting: effects of metamorphic grade and deformation on microstructures. European Journal of Mineralogy 18 (1), 21–33.

Bailey, S.W., Holdsworth, R.E., Swarbrick, R.E., 2000. Kinematic history of a reactivated oceanic structure: the Mamonia complex suture zone, SW Cyprus. Journal of the Geological Society of London 157, 1,107–1,126.

Berthé, D., Choukroune, P., Jegouzo, P., 1979. Orthogneiss, mylonite and non coaxial deformation of granites: the example of the South Armorican Shear Zone. Journal of Structural Geology 1, 31–42.

Bourdon, L., 1985. La Cordillere Orientale Dominicaine (Hispaniola, Grandes Antilles): Un Arc Insulaire Cretace Polystructure [The Cordillere Orientale Dominicaine (Hispaniola, Grandes Antilles): A Polystructural Cretaceous Island Arc]. Ph.D. thesis, Universite Pierre et Marie Curie.

Bowin, C.O., 1966. Geology of the Central Dominican-Republic (a case history of part of an island arc). In: Hess, H.H. (Ed.), Caribbean Geological Investigations. Geological Society of American Memoir. Geological Society of America, Boulder, CO, pp. 11–84.

Briggs, R.P., Akers, J.P., 1965. Hydrogeologic map of Puerto Rico and adjacent Islands. United States Geological Survey Hydrologic Investigations Atlas HA-197, scale 1:240,000.

Byrne, D.B., Suarez, G., McCann, W.R., 1985. Muertos trough subduction – microplate tectonics in the northern Caribbean? Nature 317, 420–421.

Cobiella-Reguera, J.L., 2005. Emplacement of Cuban ophiolites. Geologica Acta 3, 273–294.

Curet, A.F., 1981. The geology of a Cretaceous–Tertiary volcano–sedimentary sequence in the Mayaguez and Rosario quadrangles in west-central Puerto Rico. Ph.D. thesis, University of California, Santa Barbara.

Curet, A.F., 1986. Geologic map of the Mayagüez and Rosario quadrangles, Puerto Rico. United States Geological Survey Miscellaneous Investigations Series Map I-1657, scale 1:20,000.

Dewey, J.F., Holdsworth, R.E., Strachan, R.A., 1998. Transpression and transtension zones. In: Holdsworth, R.E., Strachan, R.A., Dewey, J.F. (Eds.), Continental Transpressional and Transtensional Tectonics. Geological Society Special Publication 135, London, pp. 1–14.

Dolan, J., Mann, P., de Zoeten, R., Heubeck, C., Shiroma, J., Monechi, S., 1991. Sedimentologic, stratigraphic, and tectonic synthesis of Eocene–Miocene sedimentary basins, Hispaniola and Puerto Rico. In: Mann, P., Draper, G., Lewis, J.F. (Eds.), Geologic and Tectonic Development of the North America-Caribbean Plate Boundary in Hispaniola. Geological Society of America Special Paper 262. Geological Society of America, Boulder, CO, pp. 217–264.

Draper, G., 1979. Tectonics of the regionally metamorphosed rocks of eastern Jamaica. Ph.D. thesis, University of the West Indies.

Draper, G., Barros, J.A., 1994. Cuba. In: Donovan, S.K., Jackson, T.A. (Eds.), Caribbean Geology: An Introduction. University of West Indies Publishers Association, pp. 65–86.

Draper, G., Gutierrez, G., Lewis, J.F., 1996. Thrust emplacement of the Hispaniola peridotite belt: orogenic expression of the mid-Cretaceous Caribbean arc polarity reversal? Geology 24 (12), 1143–1146.

Erikson, J.P., Pindell, J.L., Larue, D.K., 1990. Mid-Eocene–early Oligocene sinistral transcurrent faulting in Puerto Rico associated with formation of the northern Caribbean plate boundary zone. Journal of Geology 98 (3), 365–384.

Escuder-Viruete, J., Contreras, F., Stein, G., Urien, P., Joubert, M., Ullrich, T., Mortensen, J., Pérez-Estaún, A., 2006. Transpression and strain partitioning in the Caribbean Island-arc: fabric development, kinematics and Ar–Ar ages of syntectonic emplacement of the Loma de Cabrera batholith, Dominican Republic. Journal of Structural Geology 28 (8), 1496–1519.

García-Casco, A., Iturralde-Vinent, M., Pindell, P., 2008. Latest Cretaceous collision/accretion between the Caribbean Plate and Caribeana: origin of metamorphic terranes in the Greater Antilles. International Geology Review 50 (9), 781–809.

García-Senz, J., Monthel, J., Díaz de Neira, J.A., Hernaiz Huerta, P.P., Calvo, J.P., Escuder Viruete, J., 2007. Estratigrafía del Cretácico Superior de la Cordillera Oriental de la República Dominicana. Boletín Geológico y Minero 118 (2), 269–292.

Glover III., L., 1971. Geology of the Coamo area, Puerto Rico, and its relation to the volcanic arc-trench association. U.S. Geological Survey Professional Paper 636, 102.

Harland, W.B., 1971. Tectonic transpression in Caledonian Spitsbergen. Geological Magazine 108 (1), 27–42.

Harlow, G.E., Hemming, S.R., Lallemant, H.G.A., Sisson, V.B., Sorensen, S.S., 2004. Two high-pressure–low-temperature serpentinite-matrix melange belts, Motagua fault zone, Guatemala: a record of Aptian and Maastrichtian collisions. Geology 32 (1), 17–20.

Hess, H.H., Otalora, G., 1964. Mineralogical and chemical composition of the Mayaguez Serpentinite cores. In: Burk, C.A. (Ed.), A Study of Serpentinite: the AMSOC Core Hole near Mayaguez, Puerto Rico. National Academy of Science NSF Pub 1188, Washington, D.C, pp. 152–168.

Hernaiz-Huerta, P.P., Pérez-Estaún, A., 2002. Estructura del cinturón de pliegues y cabalgamientos de Peralta, República Dominicana. Acta Geológica Hispánica 37 (2–3), 183–205.

Jansma, P., Lopez, A., Mattioli, G., DeMets, C., Dixon, T., Mann, P., Calais, E., 2000. Microplate tectonics in the northeastern Caribbean as constrained by Global Positioning (GPS) geodesy. Tectonics 19, 1021–1037.

Jolly, W.T., Lidiak, E.G., Schellekens, J.H., Santos, H., 1998. Volcanism, tectonics, and stratigraphic correlations in Puerto Rico. In: Lidiak, E.G., Larue, D.K. (Eds.), Tectonics and Geochemistry of the Northeastern Caribbean. Geological Society of America Special Paper 322. Geological Society of America, Boulder, Colorado, pp. 1–34.

Joyce, J., 1991. Blueschist metamorphic and deformation on the Samana Peninsula – a record of subduction and collision in the Greater Antilles. In: Mann, P., Draper, G., Lewis, J.F. (Eds.), Geologic and Tectonic Development of the North America–Caribbean Plate Boundary in Hispaniola. Geological Society of America Special Paper 262. Geological Society of America, Boulder, CO, pp. 47–76.

Kamb, W.B., 1959. Ice petrofabrics observations from Blue Glacier, Washington in relation to theory and experiment. Journal of Geophysical Research 64, 1891–1909.

Krushensky, R.D., Monroe, W.H., 1978. Geologic Map of the Yauco and Punta Verraco quadrangles, Puerto Rico. United States Geological Survey Miscellaneous Investigations Series Map I-1147, scale 1:20,000.

Laó-Dávila, D.A., 2002. Middle Tertiary to recent tectonics of western Puerto Rico: paleostress and paleomagnetic study. M.S. thesis, Florida International University.

Lewis, J.F., Draper, G., Proenza, J.A., Espaillat, J., Jiménez, J., 2006. Ophiolite-related ultramafic rocks (serpentinites) in the Caribbean region: a review of their occurrence, composition, origin, emplacement and Ni-laterite soil formation. Geologica Acta 4 (1–2), 237–263.

Li, X.-P., Rahn, M., Bucher, K., 2004. Serpentinites of the Zermatt–Saas ophiolite complex and their texture evolution. Journal of Metamorphic Geology 22, 159–177.

Llerandi Román, P.A., 2004. The Geology of the western section of the Sabana Grande quadrangle: implications for the geological evolution of southwestern Puerto Rico. M.S. thesis, University of Puerto Rico.

Mann, P., Prentice, C.S., Hippolyte, J.-C., Grindlay, N.R., Abrams, L.J., Laó-Dávila, D., 2005. Reconnaissance study of Late Quaternary faulting along Cerro Goden fault zone, western Puerto Rico. In: Mann, P. (Ed.), Active Tectonics and Seismic Hazards of Puerto Rico, the Virgin Islands, and Offshore Areas. Geological Society of America Special Paper 385. Geological Society of America, pp. 115–138.

Marrett, R., Allmendinger, R.W., 1990. Kinematic analysis of fault-slip data. Journal of Structural Geology 12 (8), 973–986.

Martínez Colón, M., 2003. Geologic and tectonic history of the eastern section of the Sabana Grande quadrangle. M.S. thesis, University of Puerto Rico.
Mattson, P., 1973. Middle cretaceous nappe structures in Puerto Rican ophiolites and their relation to the tectonic history of the Greater Antilles. Geological Society of America Bulletin 84, 21–38.
Mattson, P.H., 1960. Geology of the Mayagüez area, Puerto Rico. Geological Society of America Bulletin 71, 319–362.
Mattson, P.H., 1964. Petrography and structure of serpentinite from Mayaguez, Puerto Rico. In: Burk, C.A. (Ed.), A Study of Serpentinite: The AMSOC Core Hole near Mayaguez, Puerto Rico. National Academy of Science NSF Pub 1188, Washington, D.C., pp. 7–24.
Mattson, P.H., Schwartz, D.P., 1971. Control of intensity of deformation in Puerto Rico by mobile serpentinized peridotite basement. In: Donnelly, T.W. (Ed.), Caribbean Geophysical, Tectonic, and Petrologic Studies. Geological Society of America Memoir 130, Colorado, Boulder, pp. 97–106.
McIntyre, D.H., 1975. Geologic Map of the Maricao Quadrangle, Puerto Rico. United States Geological Survey Miscellaneous Investigations Series map I-918, scale 1:20,000.
Monroe, W.H., 1980. Some tropical landforms of Puerto Rico. U.S. Geological Survey Professional Paper 1159, 39.
Montgomery, H., Pessagno, E., Pindell, J.L., 1994. A 195 Ma terrane in a 165 Ma sea: Pacific origin of the Caribbean Plate. GSA Today 4 (1), 1–6.
Mori, R., Ogawa, Y., 2005. Transpressional tectonics of the Mineoka Ophiolite Belt in a trench–trench–trench-type triple junction, Boso Peninsula, Japan. The Island Arc 14, 571–581.
Nagle, F., 1974. Blueschist, eclogite paired metamorphic belts and the early tectonic history of Hispaniola. Geological Society of America Bulletin 85, 1461–1466.
Nozaka, T., 2005. Metamorphic history of serpentinite mylonites from the Happo ultramafic complex, central Japan. Journal of Metamorphic Geology 23, 711–723.
O'Hanley, D.S., 1992. Solution to the volume problem in serpentinization. Geology 20, 705–708.
O'Hanley, D.S., 1996. Serpentinites: Records of Tectonic and Petrological History. Oxford University Press, New York.
Pindell, J.L., 1994. Evolution of the Gulf of Mexico and the Caribbean. In: Donovan, S.K., Jackson, T.A. (Eds.), Caribbean Geology: An Introduction. University of West Indies Publishers Association, pp. 13–39.
Reid, J.A., Plumley, P.W., Schellekens, J.H., 1991. Paleomagnetic evidence for Late Miocene counterclockwise rotation of North Coast carbonate Sequence, Puerto Rico. Geophysical Research Letters 18 (3), 565–568.
Santos, H., 1999. Stratigraphy and depositional history of the upper Cretaceous strata in the Cabo Rojo–San German structural block, southwestern Puerto Rico. Ph.D. thesis, University of Colorado.
Santos, H., 2005. Stratigraphy and depositional history of the upper Cretaceous strata in southwestern. Geological Society of America Abstracts with Programs 37 (7), 370.
Schellekens, J.H., 1998. Composition, metamorphic grade, and origin of metabasites in the Bermeja Complex, Puerto Rico. International Geology Review 40 (8), 722–747.
Schwartz, D.P., 1970. The geology of the Punta Guanajibo–Cuchilla Sabana Alta area, western Puerto Rico. M.A. thesis, Queens College, The City University of New York.
Slowdowski, T.R., 1956. Geology of the Yauco area, Puerto Rico. Ph.D. thesis, Princeton University.
Stuart-Smith, P.G., 1990. The emplacement and fault history of the Coolac Serpentinite, Lachlan Fold Belt, southeastern Australia. Journal of Structural Geology 12 (5/6), 621–638.
Tobisch, O.T., 1968. Gneissic amphibolite at Las Palmas, Puerto Rico, and its significance in the early history of the Greater Antilles island arc. Geological Society of America Bulletin 79, 557–574.
Twiss, R., Gefell, 1990. Curved slickenfibers: a new brittle shear sense indicator with application to a sheared serpentinite. Journal of Structural Geology 12, 471–480.
Twiss, R., Protzman, G.M., Hurst, S.D., 1991. Theory of slickenline patterns based on the velocity gradient tensor and microrotation. Tectonophysics 186, 215–239.
Twiss, R., Unruh, J.R., 1998. Analysis of fault slip inversions: do they constrain stress or strain rate? Journal of Geophysical Research 103 (B6), 12,205–12,222.
van Fossen, M.C., Channell, J.E.T., Schellekens, J.H., 1989. Paleomagnetic evidence for Tertiary anticlockwise rotation in southwest Puerto Rico. Geophysical Research Letters 16, 819–822.
Volckmann, R.P., 1984a. Geologic Map of the Cabo Rojo and Parguera quadrangles, southwest Puerto Rico. United States Geological Survey Miscellaneous Investigations Series Map I-1557, scale 1:20,000.
Volckmann, R.P., 1984b. Geologic Map of the Puerto Real quadrangle, southwest Puerto Rico. United States Geological Survey Miscellaneous Investigations Series Map I-1559, scale 1:20,000.
Volckmann, R.P., 1984c. Geologic Map of the San German quadrangle, southwest Puerto Rico. United States Geological Survey Miscellaneous Investigations Series Map I-1558, scale 1:20,000.
Wadge, G., Draper, G., Lewis, J.F., 1984. Ophiolites of the northern Caribbean: a reappraisal of their roles in the evolution of the Caribbean plate boundary. In: Gass, I.G., Lippard, S.J., Shelton, A.W. (Eds.), Ophiolites and Oceanic Lithosphere. Blackwell Scientific Publications, Oxford, pp. 367–380.
Wojtal, S., 2001. The nature and origin of asymmetric arrays of shear surfaces in fault zones. In: Holdsworth, R.E., Strachan, R.A., Magloughlin, J.F., Knipe, R.J. (Eds.), The Nature and Tectonic Significance of Fault Zone Weakening. Geological Society. Special Publications 186, London, pp. 171–193.
Wojtal, S., Mitra, G., 1988. Nature of deformation in some fault rocks from Appalachian thrusts. Geological Society of America Special Paper 222, pp. 17–33.